HURRICANE HILDA, 1964

I. GENESIS, AS REVEALED BY SATELLITE PHOTOGRAPHS, CONVENTIONAL AND AIRCRAFT DATA

HARRY F. HAWKINS and DARYL T. RUBSAM

National Hurricane Research Laboratory, Research Laboratories, ESSA, Miami, Fla.

ABSTRACT

The formation of hurricane Hilda is followed using satellite photographs, surface and 200-mb. streamline analyses, and 500- to 200-mb. thickness and shear wind analyses. The formation of a strong upper level anticyclone nearly over the perturbation coincided with marked warming in the 500- to 200-mb. level. Significant deepening was delayed until the disturbance was clear of the island of Cuba. Profiles of meteorological parameters are studied as the deepening proceeds and details of the structure from photographs and radar film are presented.

1. INTRODUCTION

Hilda was a late season storm, the first sign of which appeared at the surface as a weak wave in the easterlies over eastern Cuba on Sept. 27, 1964. The wave proceeded slowly westward deepening into a closed Low on the 29th, and maintained its intensity as it crossed over the southwestern peninsula of Cuba by the 30th. In the western Yucatan channel it began to deepen more rapidly, and while moving west-northwestward through the Gulf of Mexico it reached hurricane strength about 16 GMT on September 30. Hilda attained its maximum intensity (central pressure of 941 mb.) around 19 GMT on October 1 after which it proceeded slowly toward the north to the Louisiana coastline while filling at a moderate rate. The eye of Hilda passed over Franklin, La. (some 10 mi. inland), about 03 GMT on October 4. The central pressure was 962 mb. and the winds were estimated at 135 mi./hr. (Dunn et al. [1]). Following this report, the storm filled rapidly and turned northeastward and eastward before an approaching cold front. It became extratropical over southern Mississippi and produced heavy rains in the Southeast as it passed to sea off the coast near Jacksonville, Fla. (In eastern North Carolina, some 4,000 persons had to evacuate their homes because of flooding (Frank [4]).)

During its formative stages the incipient perturbation could be analyzed fairly well using the Caribbean synoptic reports despite the absence of upper air soundings from Havana and Camaguey, Cuba. On September 29 and 30 and again on October 1 and 2, special research flights by the National Hurricane Research Laboratory—Research Flight Facility team—made Hilda one of the best documented storms in history. The upper level flights were indispensible in the 200-mb. streamline analyses. On the 1st, special efforts were made to gather data at five levels from the still deepening hurricane. These data provided the best vertical resolution obtained to that date in the inner core of a hurricane.

The two major purposes of this paper, which is being published in three parts, are to describe the formation of Hilda in all available detail and to examine the storm on the 1st in as many relevant ways as the aircraft data permit. A somewhat more cursory discussion of the approach of the storm to the coast and its degradation into an extratropical wave are finally presented. The authors have endeavored to use satellite photographs where they appear helpful and informative.

2. THE FORMATION OF HURRICANE HILDA

The official track of hurricane Hilda is presented in figure 1, which shows that the storm was first recorded as a tropical depression at 12 GMT on Sept. 28, 1964. However, the first notice that a possible disturbance was forming out over the Atlantic was contained in a message from the National Weather Satellite Center on Sept. 23, 1964. TIROS 7 had detected an amorphous mass of clouds characterized as a "disturbed area." Available surface weather reports did not indicate any significant perturbation in the low level flow field and there were insufficient data aloft to define the analysis. Late on the 24th (fig. 2) a subsequent picture showed either westward motion of the cloud formation or a newly formed cloud mass. Few useful data were available at sea level, and at 200 mb. there was a suggestion that the cloud mass was centered near the south side of a col. The 500-mb. analysis (not shown) was quite similar to that at 200 mb. One day later the cloudiness was centered farther west and appeared much more extensive (fig. 3). At the 200-mb. level it seemed to be located throughout the col and the easterly wave south of the col; at 500 mb. the axis of a fairly strong easterly wave was about 2° of long. west of the 200-mb. axis.

On September 26, no satellite picture was available, but by 00 GMT on the 27th a closed cyclonic circulation had developed over Haiti at the upper level (fig. 4) and a barely detectable wave in the easterlies could be analyzed

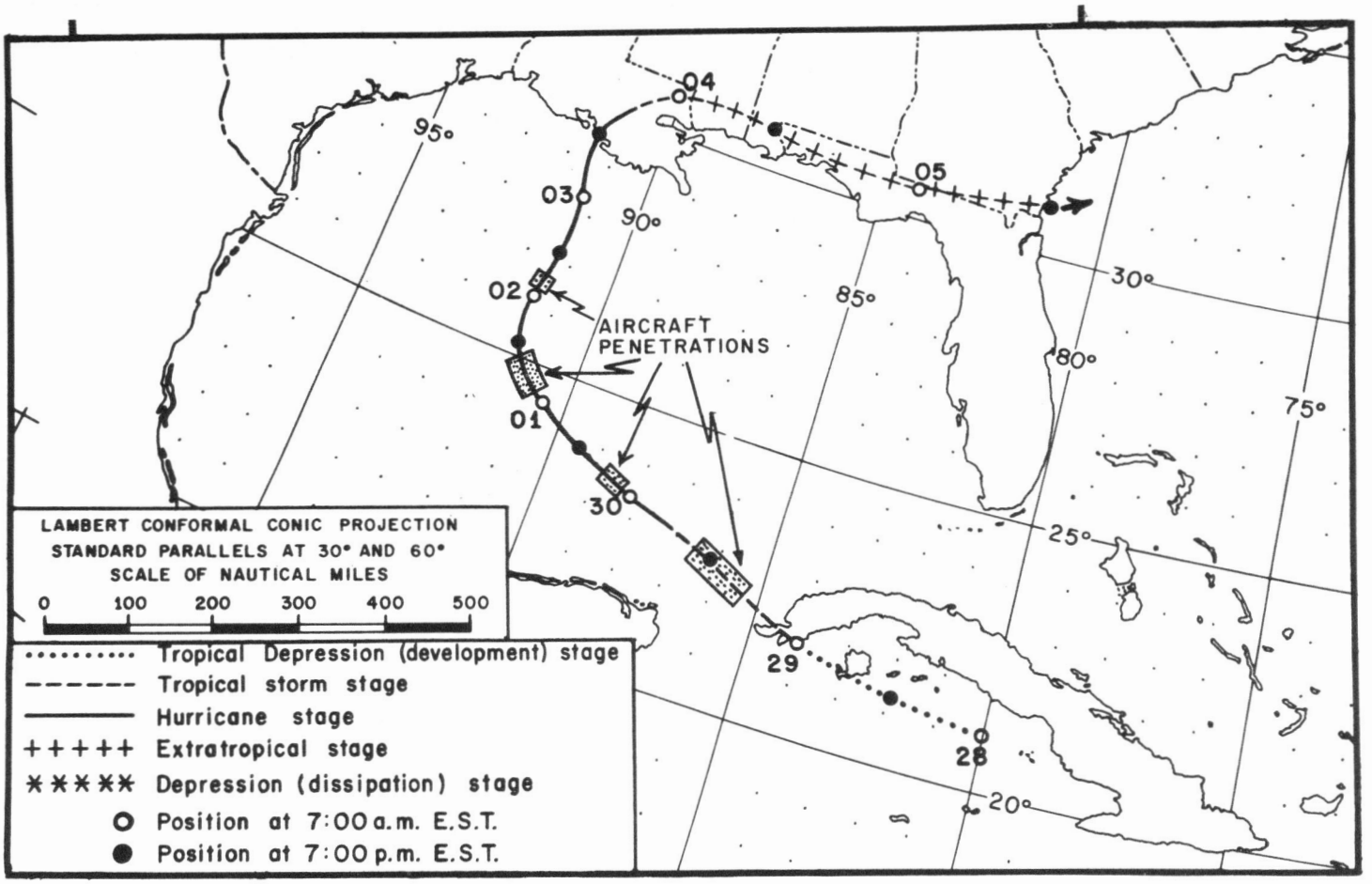

FIGURE 1.—The track of hurricane Hilda, Sept. 28–Oct. 5, 1964, including tropical depression, tropical storm, hurricane and extratropical phase stages.

over eastern Cuba at the surface (fig. 5). The connection between these two features was rather tenuous, as evidenced by the relation of the surface trough to the 500- to 200-mb. thickness pattern (fig. 6) and the subsequent history of this relationship. Twenty-four hr. later (fig. 7) the upper level vortex had moved south-southwestward and the strengthened surface wave (fig. 8) now lay under the weak thickness ridge (fig. 9). The major changes that had occurred in this period appeared to be the strengthening of the cyclonic vorticity center over the Bahamas (fig. 3) into a closed cyclonic circulation north of Cuba (fig. 7), the strengthening of the surface wave already mentioned, and the amplification of the ridge-trough thickness pattern from central to eastern Cuba (fig. 9). The thickness pattern was reasonably well supported by the shear winds, and the thickness ridge over eastern Cuba may have been partially induced by the release of latent heat in the shower activity that accompanied the wave.

The satellite photo (fig. 10) and its nephanalysis (fig. 11) covered the northern portion of the surface wave only. It did, however, suggest the development of a significant cloud mass, which appeared to have cirrus outflow oriented along the 200-mb. streamlines that diverged from the anticyclone north of Haiti (dashed lines, fig. 11). The *surface winds* and weather at reporting stations are also depicted in figure 11. The northwestern edge of the "continuous" cloud mass seemed to be defined or limited by the strong shear line extending northeastward from the cyclonic center just north of Cuba.

During the next 24 hr. a closed cyclonic vortex (at the surface) formed just to the south of Cuba. Figure 12 for 00 GMT on the 29th shows this rather large, weak, tropical depression at sea level. The 200-mb. data were significantly enhanced by the addition of the aircraft winds (fig. 13). They revealed that the major upper level anticyclone that had been north of Haiti (fig. 7) had moved over Haiti. At the same time, a new strongly divergent anticyclone had appeared near north central Cuba. During the same period the cyclonic circulation to the west (fig. 7) had degenerated into little more than a shear line.

The most impressive change occurred in the thickness pattern (fig. 14). A large mass of warmer than normal air (from 500 to 200 mb.) now covered western Cuba. Presumably this upper level warmth resulted from the release of latent heat that accompanied the slowly deepening surface disturbance. Both the warm pool and the associated cloud mass (fig. 15) were located mainly to the east of the surface low center, possibly because the disturbance had only recently developed from an easterly wave with most of the weather expected on its east side, into a closed Low, in which the weather might be expected to be distributed more symmetrically. In figure 16 there

308-679 O - 68 - 4

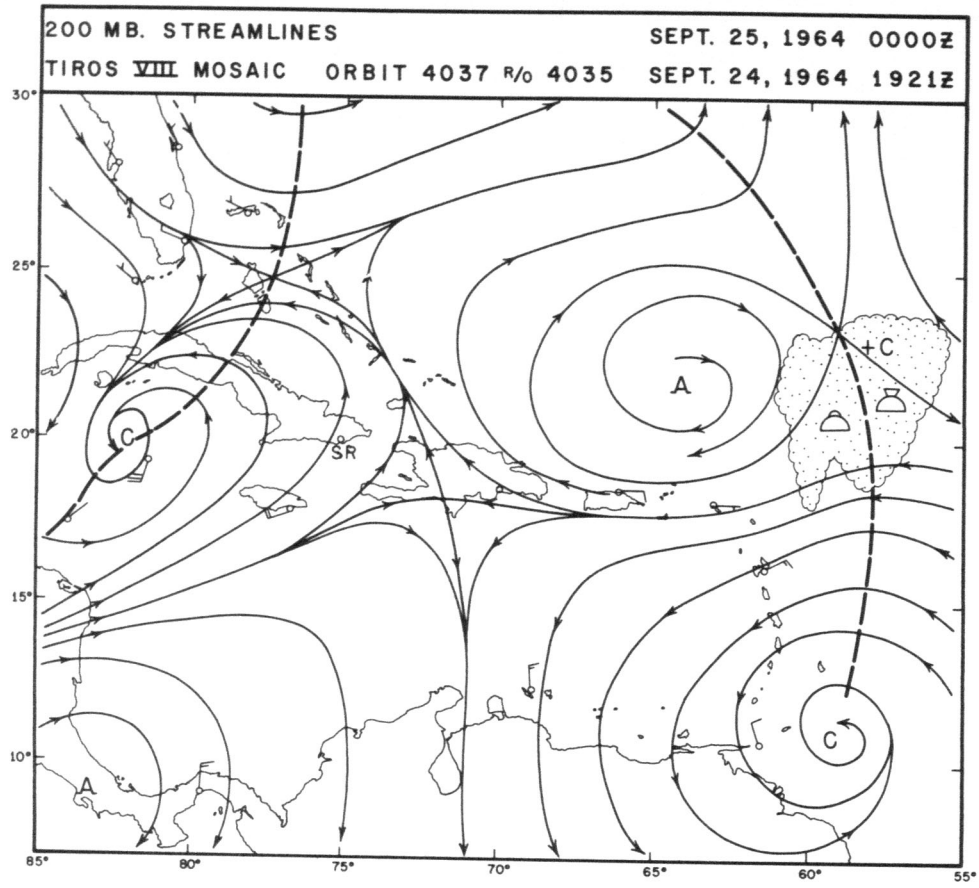

FIGURE 2.—Possible antecedent cloud mass on background of upper level streamlines for 00 GMT, September 25.

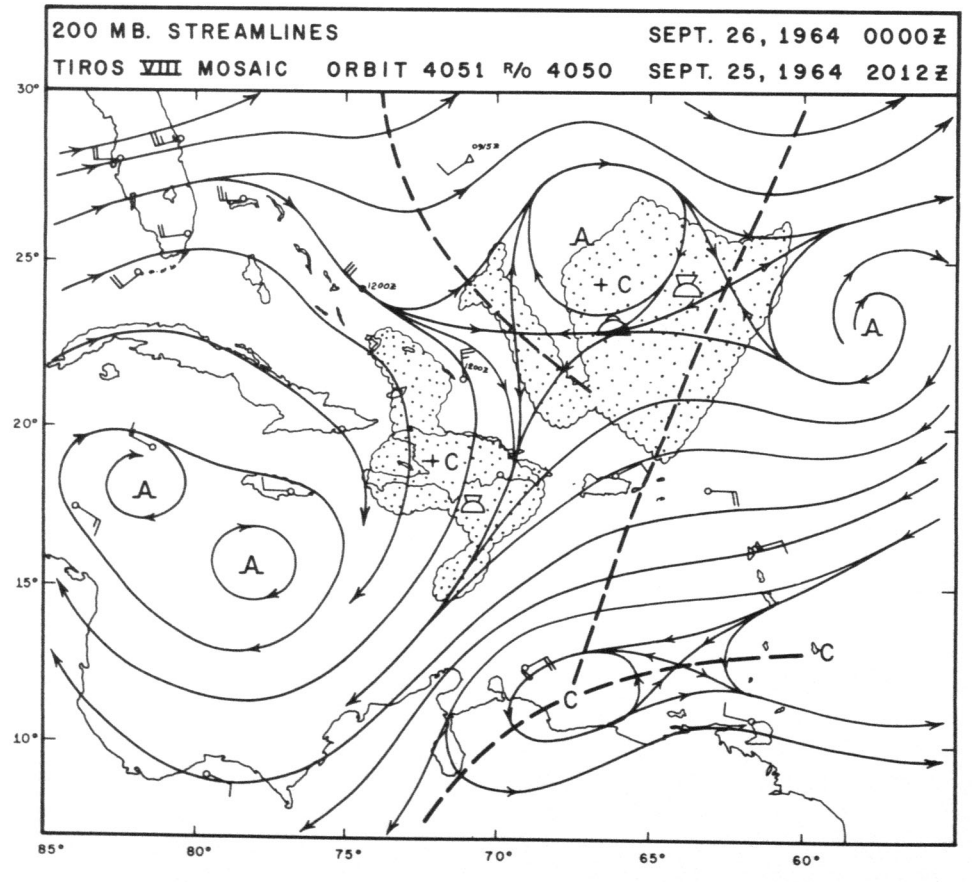

FIGURE 3.—Same as figure 2 but with more extensive cloud masses not uniquely related to upper level flow for 00 GMT, September 26.

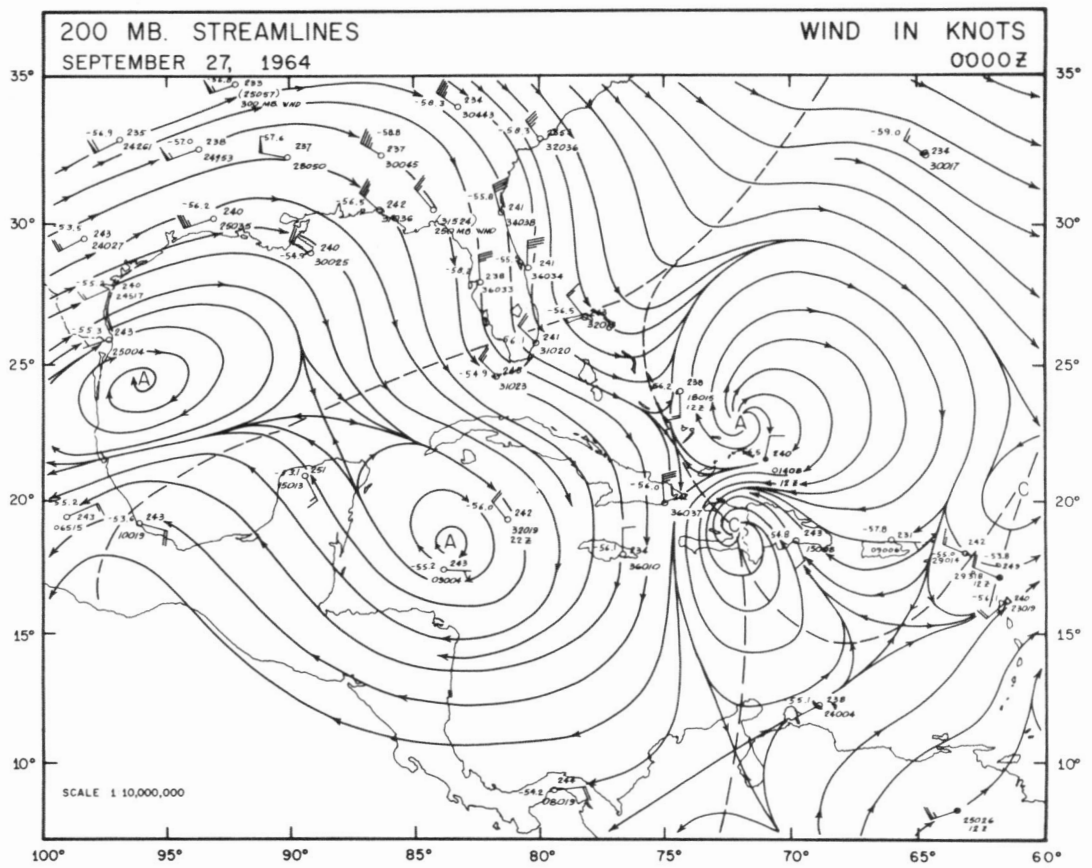

FIGURE 4.—Development of cyclonic vortex over Haiti and trough in the Bahamas.

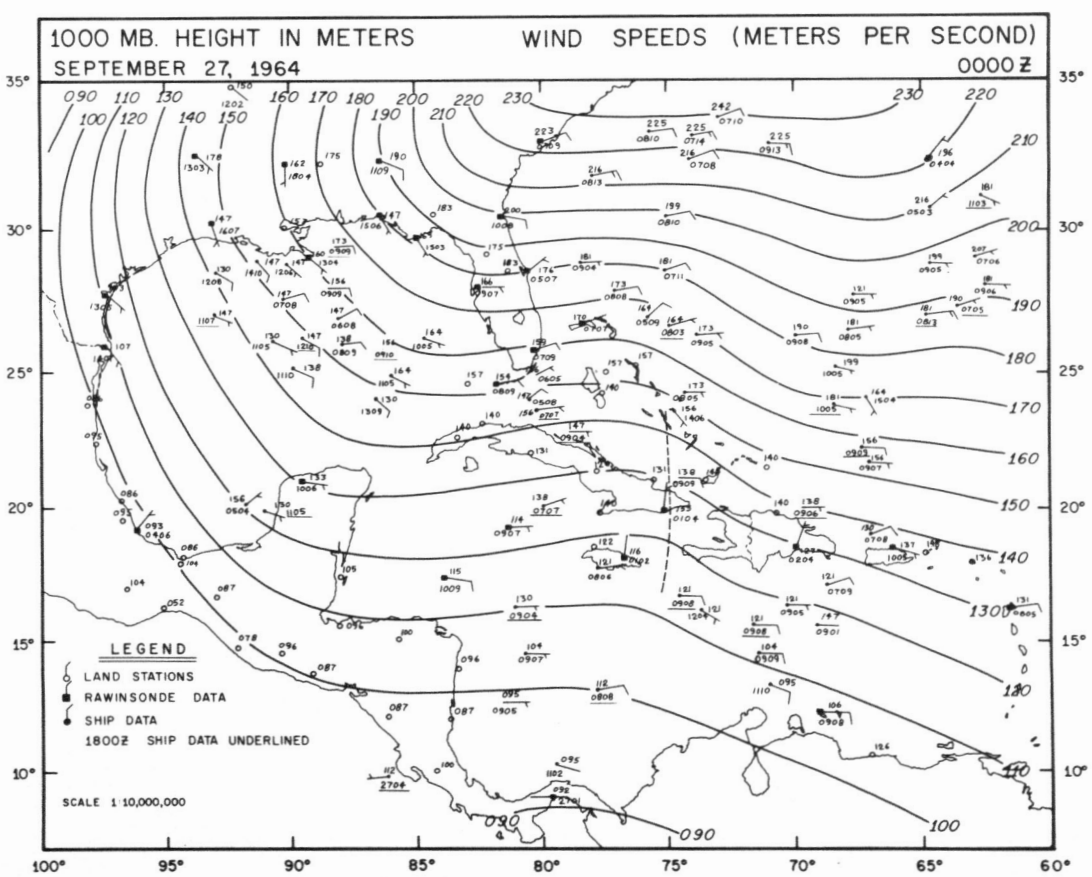

FIGURE 5.—1000-mb. contours for 00 GMT, September 27 showing a barely perceptible easterly wave over eastern Cuba, the first low level evidence of the disturbance that became hurricane Hilda.

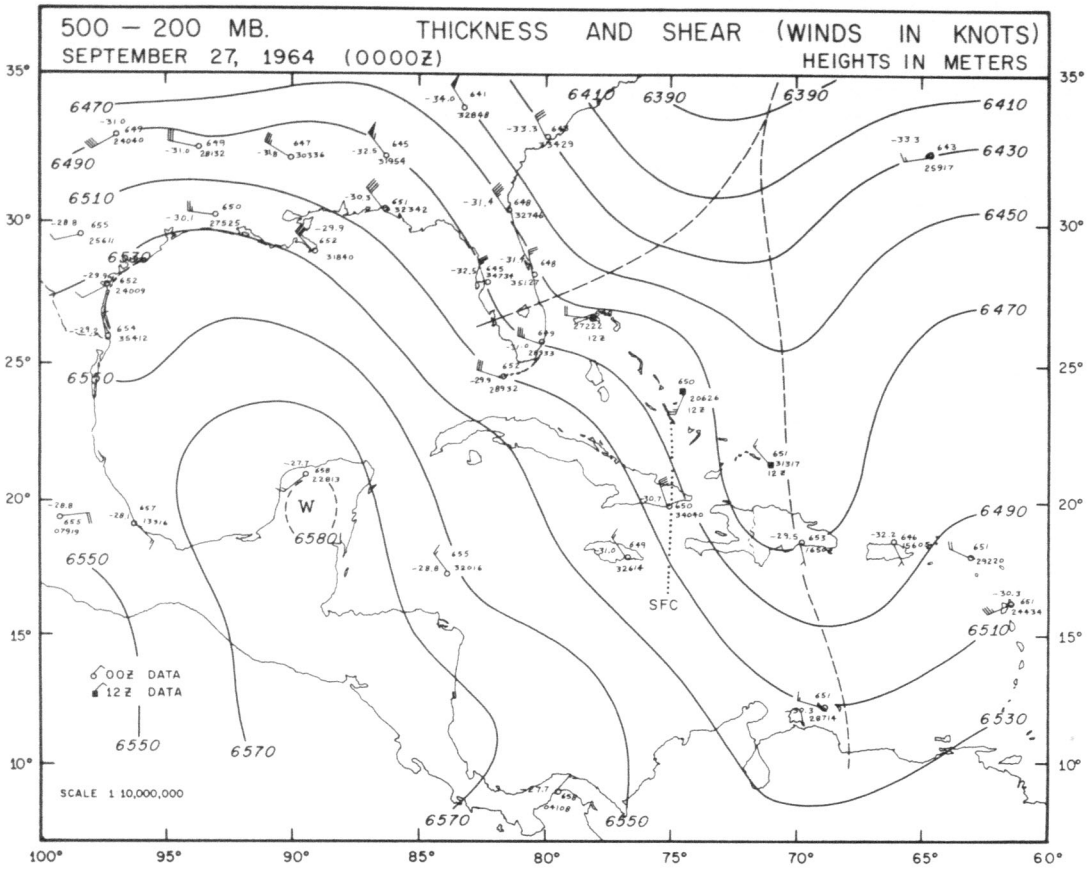

FIGURE 6.—The surface trough (dotted) almost midway between the trough-ridge system in the 500- to 200-mb. thickness.

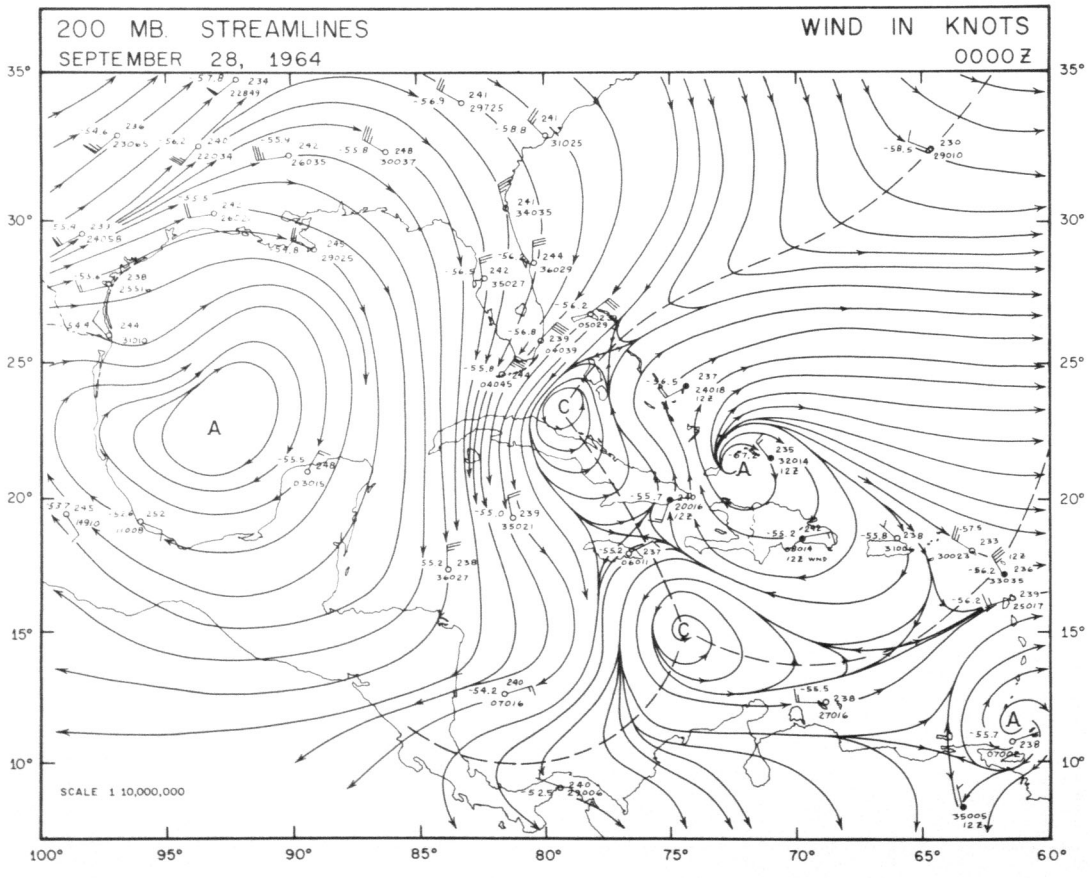

FIGURE 7.—Development of the new upper level vortex between Cuba and the Bahamas.

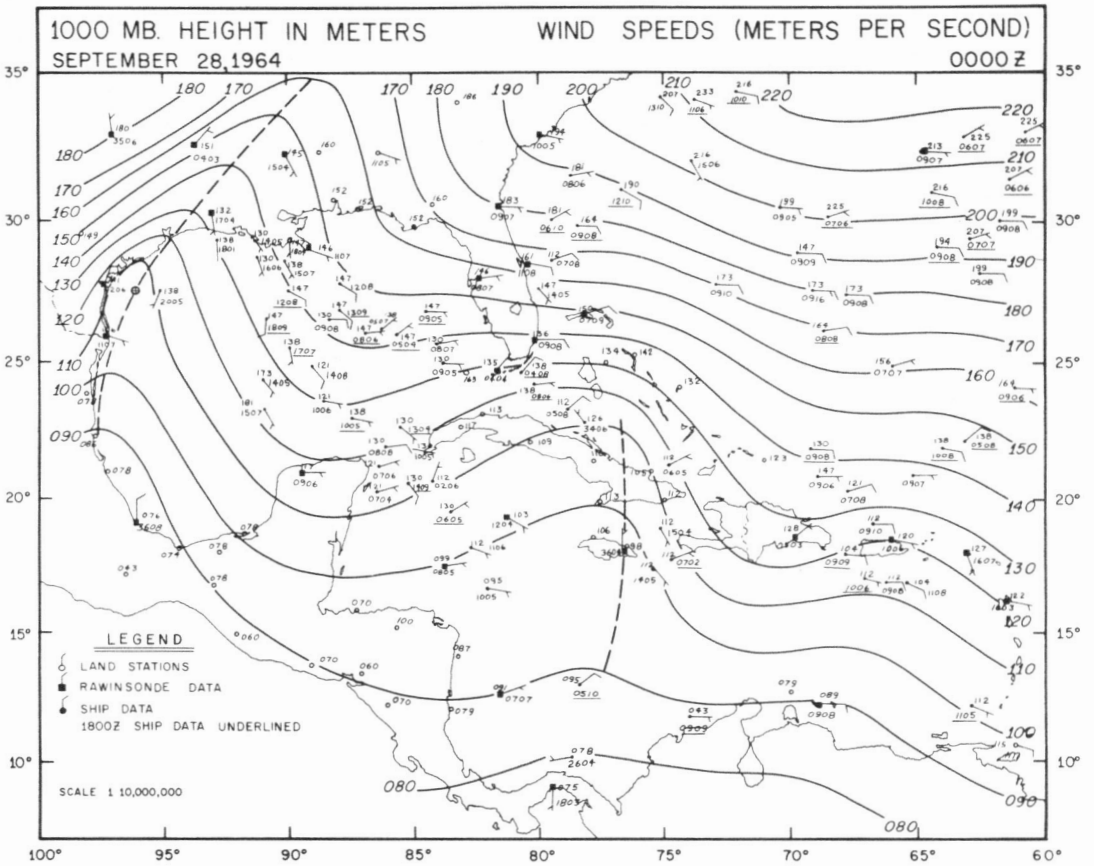

FIGURE 8.—Developing easterly wave over eastern Cuba and Jamaica.

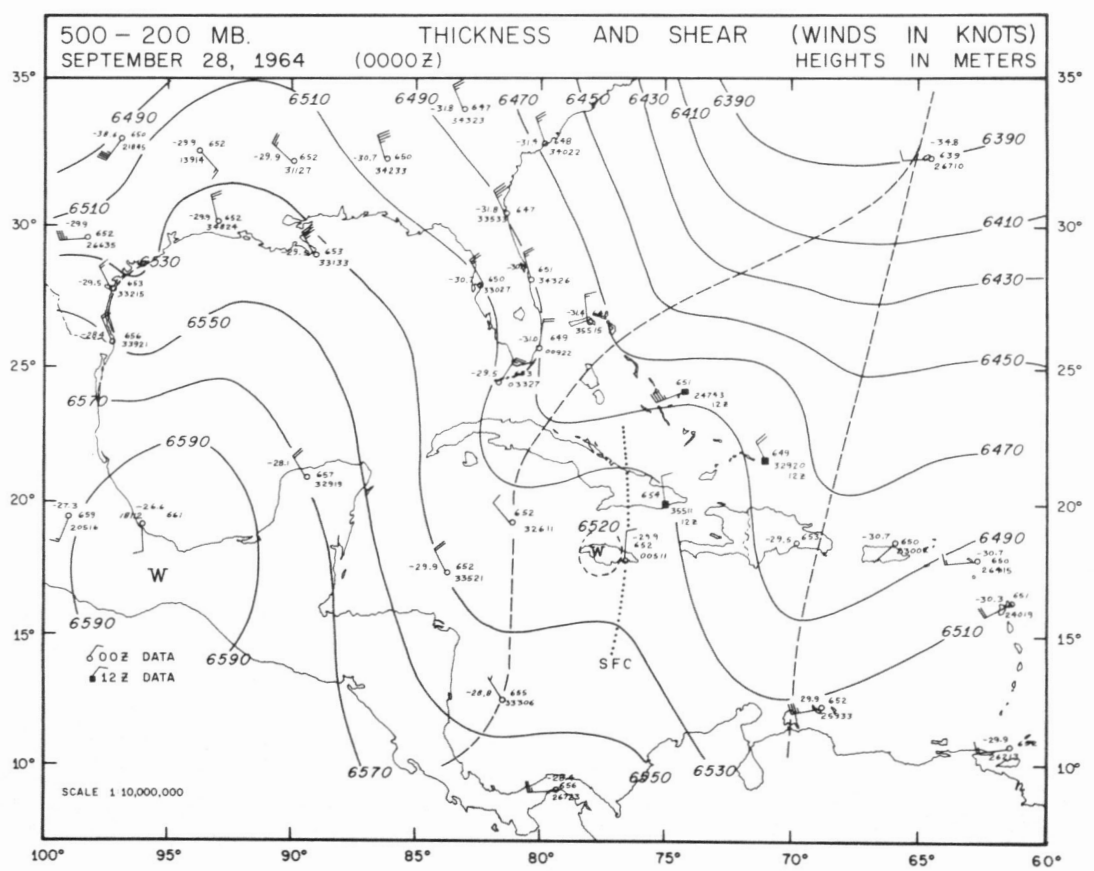

FIGURE 9.—Surface trough (dotted) now located in the 500- to 200-mb. thickness ridge.

FIGURE 10.—Satellite view of cloud masses (lower portion of picture) that preceded hurricane Hilda.

is still a suggestion that the cloudiness tends to be limited by the shear line; the edge is not particularly sharp, however, and the nephanalysis does not portray the thinner cirrus elements of figure 15. A secondary cloud mass to the north of eastern Cuba appears to have been intimately connected with these features but is not quite part of the continuous cloud mass.

Fett [3] has cataloged four typical stages of hurricane development as characterized by cloud photographs obtained from satellites. Figure 10 did not present adequate coverage for satisfactory classification along the lines suggested by him, although it does suggest a possible "A" stage of development. The coverage of figure 15 is more complete and the cloud configuration presumably falls in Fett's "C" or "B-C" category. A clear-cut "comma" configuration is rather difficult to discern.

By 00 GMT on the 30th the center at 1000 mb. had crossed western Cuba near Cabo de San Antonio (fig. 17) and was centered in the northern Yucatan passage. The storm had deepened very little but had achieved tropical storm status (12 GMT, Sept. 29) by virtue of 35-kt. winds in the northeastern sector. At 200 mb. (fig. 18) the

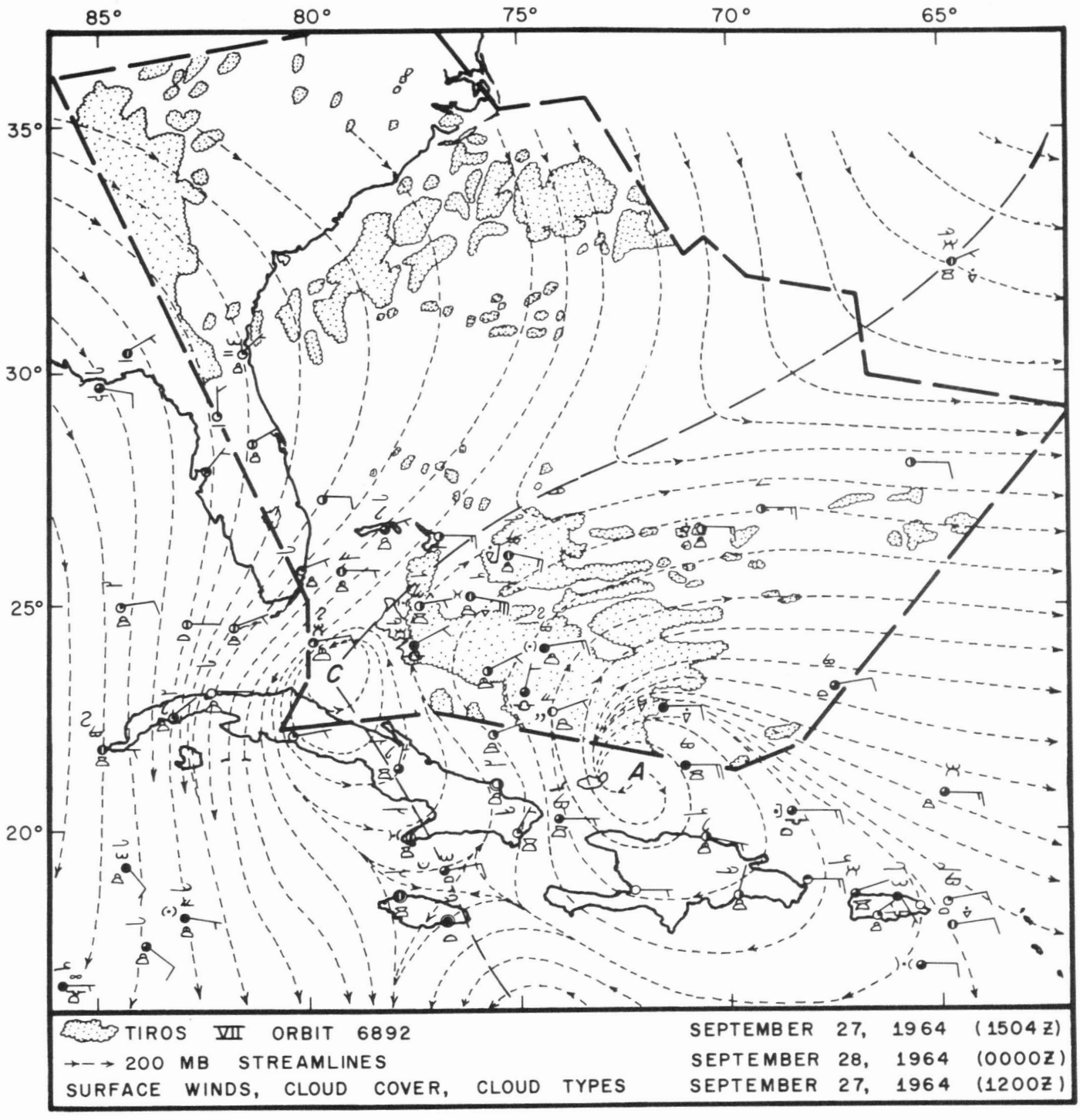

FIGURE 11.—Nephanalysis of figure 10 superimposed on the 200-mb. streamlines (9 hr. later) and the *surface winds* (3 hr. earlier).

attendant anticyclone was well delineated by the aircraft winds which showed it had moved westward as it accompanied the incipient Hilda. Between the High and the southern Florida peninsula, these reports defined a sharp shear line. Visible evidence of the shear was observed by the senior author on a research flight that same day (the 30th). The well-defined edge of the cirrus shield mapped on the low level flight coincided almost exactly with the shear line determined from the upper level flight winds that became available later. Unfortunately, the TIROS picture coverage does not extend quite far enough north to provide satellite confirmation of this observation.

Despite the lack of significant change in central pressure, the portion of the storm visible on the satellite coverage appeared much better organized on September 29 than on previous days (fig. 19). The cloud mass visible in the photograph suggests a classical "comma" corresponding to Fett's "C" stage, nominally attended by winds of 20 to 30 kt. The cloud shows strong evidence of anticyclonic outdraft in the southern section of the storm.

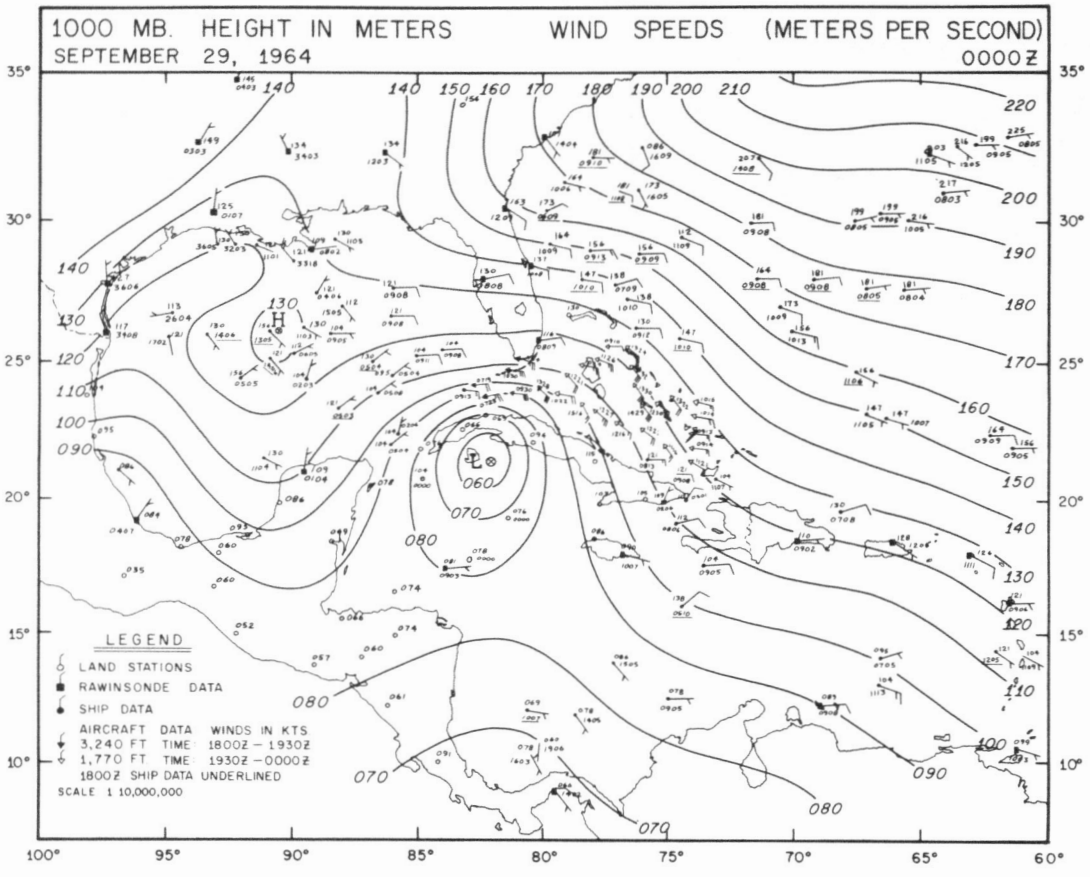

FIGURE 12.—Tropical depression (Hilda) at 00 GMT, September 29.

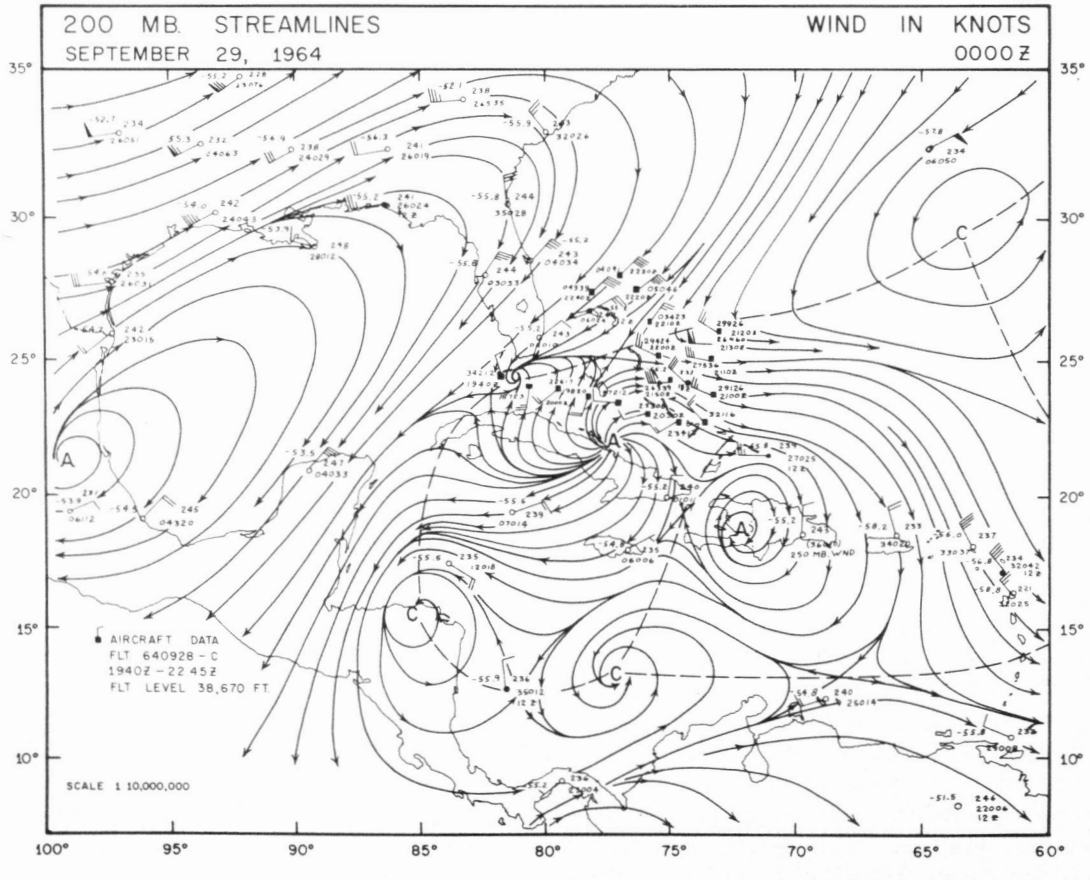

FIGURE 13.—A strongly divergent anticyclonic circulation has developed just north of Cuba as the cyclonic circulation in the Florida Straits was suppressed.

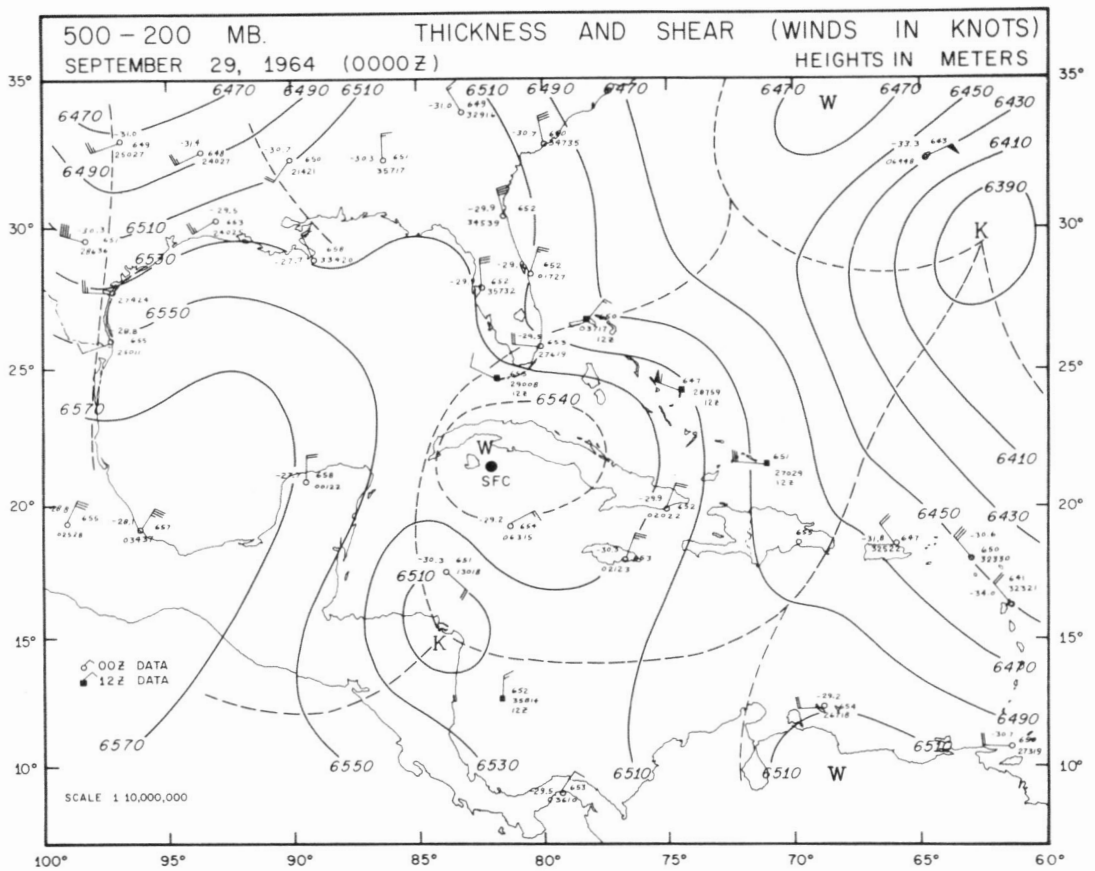

FIGURE 14.—Further marked warming in the 500- to 200-mb. layer. Shear winds clearly define the presence of anomalous warmth.

These upper level streamers appear to merge towards the west and southwest (fig. 20). In view of the difficulties in compositing the mosaic and the difference in synoptic times between the photograph and the 200-mb. streamlines, we feel the agreement is reasonably good.

The thickness map for 00 GMT on the 30th (fig. 21) suffers somewhat from scarcity of data. Nevertheless, the gross or large features are fairly well defined and certainly suggest that in the overall vicinity of the storm, thicknesses continued to increase in the layer from 500 to 200 mb. Presumably, the "separate" area of warmth present on the previous day had fused or amalgamated with the normal center of greatest warmth usually located over southern Mexico. There was every suggestion that heating was continuing in the upper levels much in the fashion described by Yanai [16], [17] in his now classical study of typhoon Doris (1958).

Of possible significance is that the heat release was strongly evident and preceded the rapid deepening despite the fact that there was no immediate cold vortex (above the low level center) that required transformation into a warm core vortex. The nearest vortex that might have been associated with Hilda in this context appears to have been the one south of Florida at 00 GMT on the 28th (fig. 7). One might have expected that deepening would accelerate rapidly following the conditions reflected in the 00 GMT maps of the 29th (fig. 12, 13). Certainly most of the generally conceded prerequisites were present: a low level disturbance (with low level inflow), an upper divergence mechanism, warm surface waters beneath, and general warmth in the 500- to 200-mb. layer. It may well be that proximity to the island of Cuba and the considerable obstacle that its terrain presents, as well as the curtailment of available water surface which the island's very presence necessitates, were sufficient deterrents to an otherwise favorable situation. The storm began to deepen at an accelerating pace shortly after 12 GMT on the 29th (fig. 22) as the storm center cleared the Cuban peninsula (Guanahacabibes), and the most rapid deepening occurred after the storm was well at sea.

Gray [5] recently studied tropical storm formation on a global scale. He came to the conclusion that formation is greatly favored over those regions where low level convergence lies beneath a deep layer (850 to 200 mb.) characterized by very little wind shear. Presumably, this prevents the latent heat released from being so widely disseminated as to make its cumulative effect nil. With this in mind, we have analyzed the 850- to 200-mb. shear winds over the region of concern. Because our prime area of interest was over the southern coast of western Cuba (which contained no upper level reporting stations), the only possible confirmation would lie in a minimum shear over this area implied by the data from surrounding areas. To a limited extent this did appear to be the case; i.e., the area about the center was in a region of relatively weak shear. The evidence was not conclusive and is not presented here.

In recent years surface water temperatures have received considerable attention as factors influencing the formation, intensification, and motion of hurricanes.

308-679 O - 68 - 5

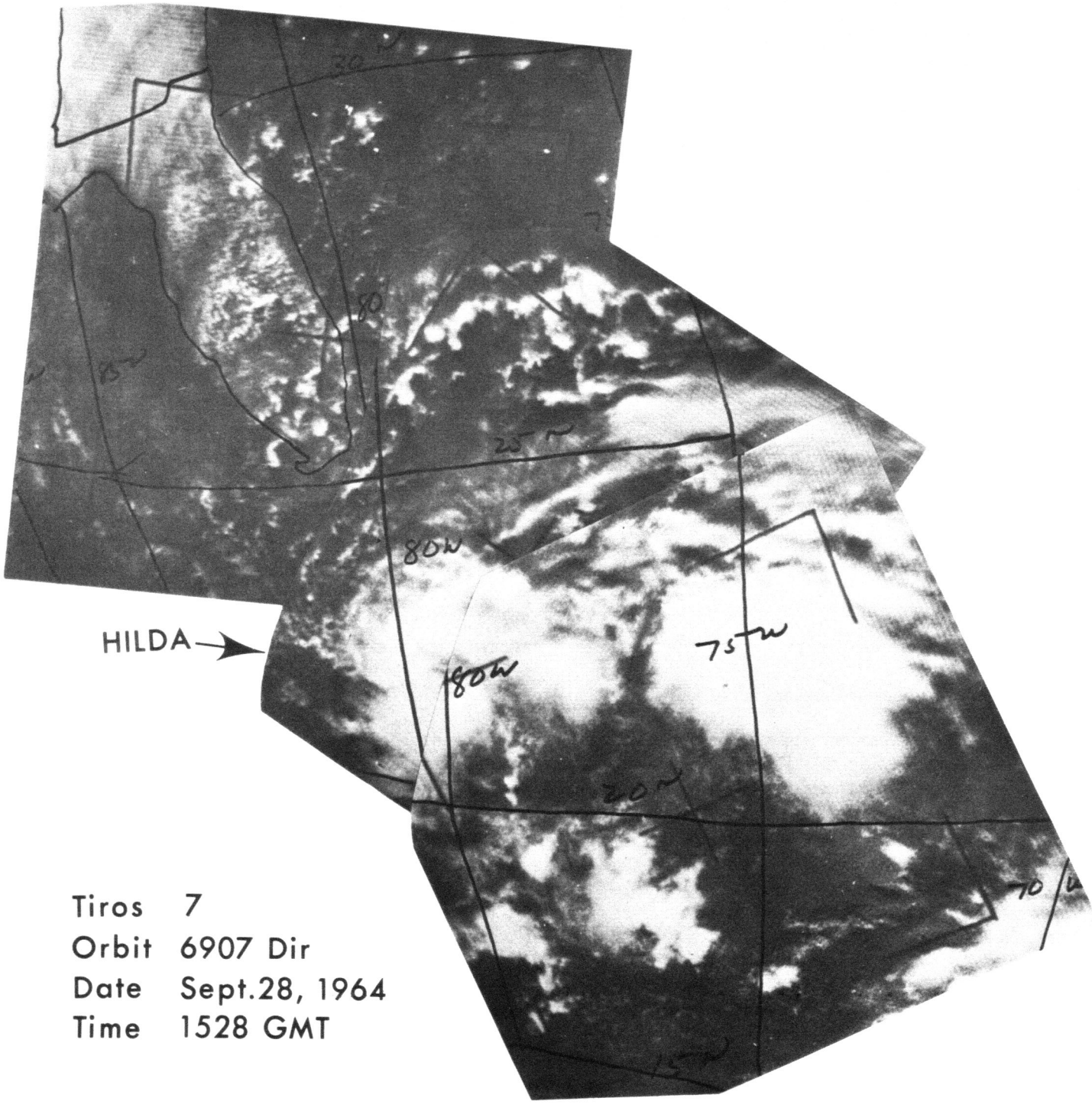

FIGURE 15.—Satellite view of the area of concern at 1528 GMT, September 28.

(Palmén [11] has long since disclaimed any intent of stating that hurricanes and typhoons can form *only* over waters of at least 26 to 27°C.) Since there was little doubt that sea surface temperatures south of Cuba were of the order of 28 to 29°C., more than adequate heat and moisture (for the over-water portion of the storm) were available long before rapid deepening began. Out over the open Gulf where the significant deepening took place, the waters were apparently just as warm or warmer. Leipper [9] and Taylor [15] have constructed detailed isotherms of the water temperatures over the Gulf before and after the passage of Hilda. A good portion of these data was gathered by an oceanographic vessel and may be considered more accurate than the usual synoptic reports. Temperatures in front of Hilda were around 29 to 30°C., or somewhat above normal for the time of year. Thus, sea surface temperature conditions were ideal for storm development.

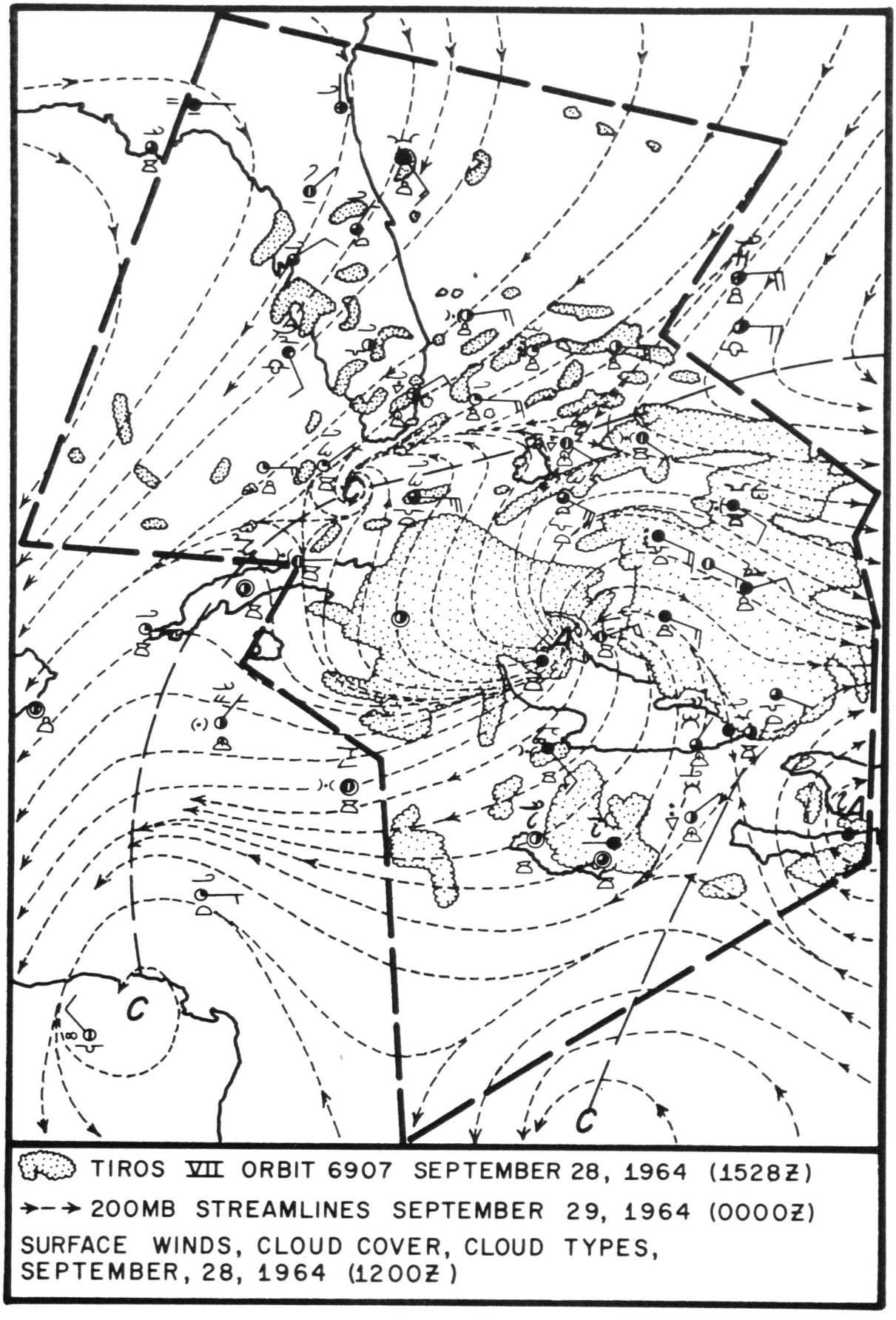

FIGURE 16.—Nephanalysis of figure 15 with 200-mb. streamlines and surface observations.

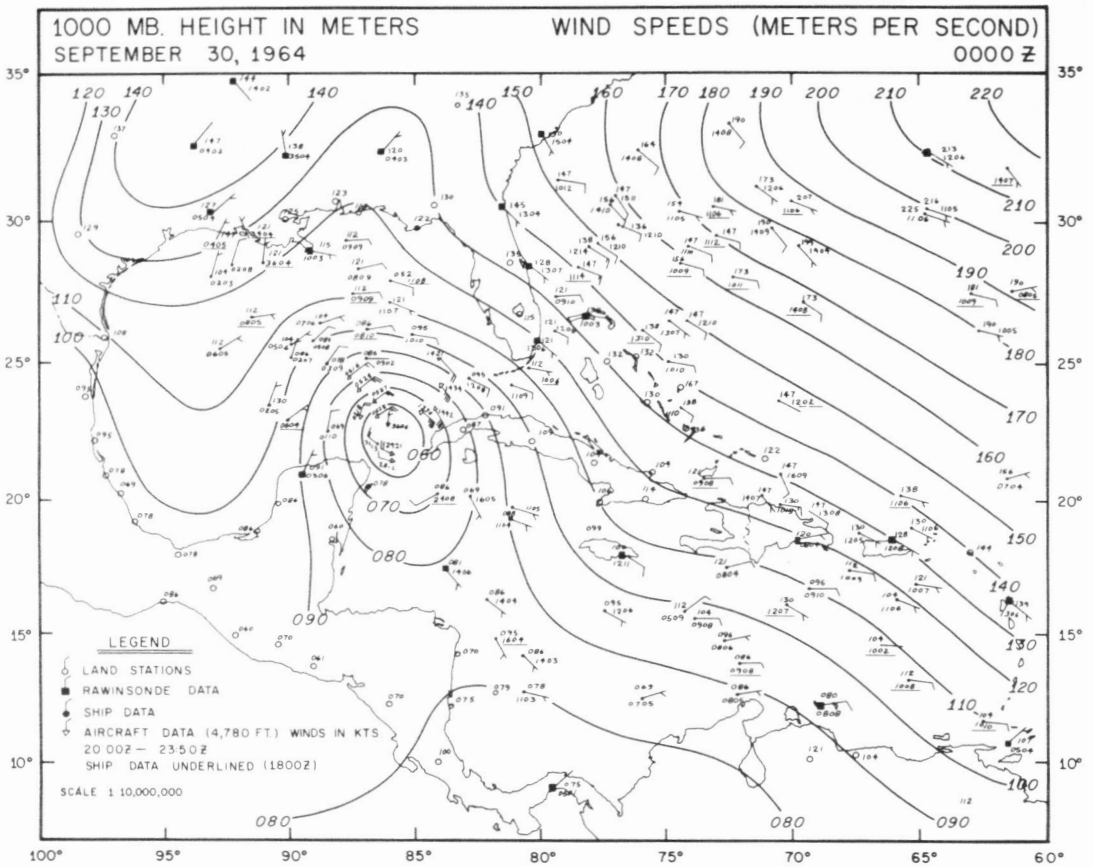

FIGURE 17.—Tropical storm Hilda at 00 GMT, September 30.

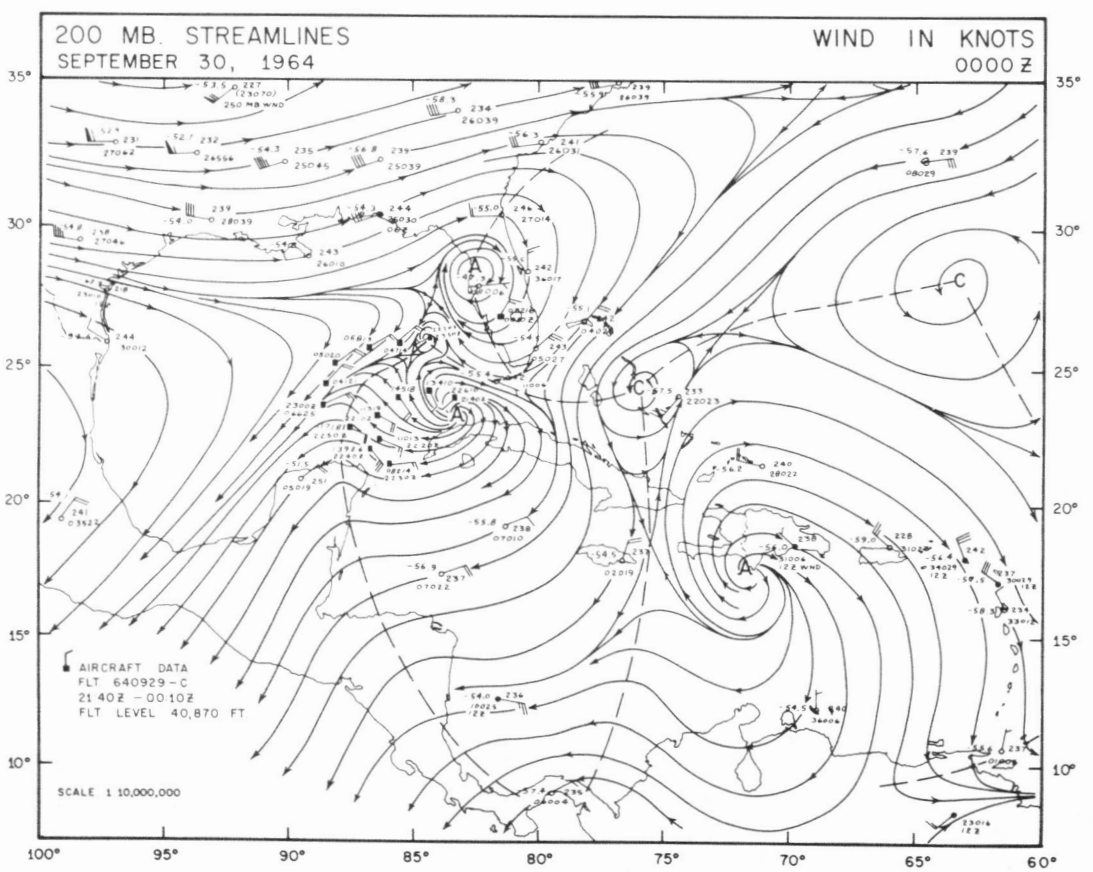

FIGURE 18.—The 200-mb. anticyclone has just about maintained its position relative to the surface perturbation.

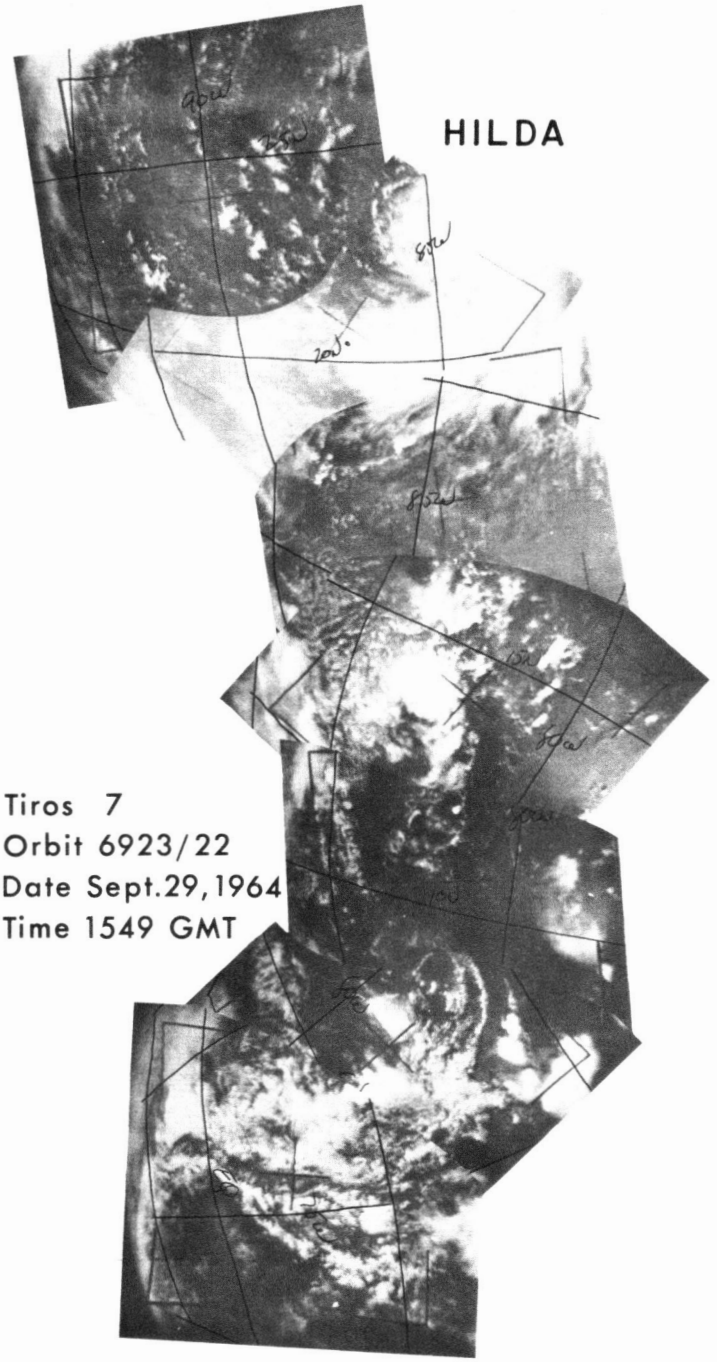

FIGURE 19.—A marked improvement in organization over a 24-hr. period. The "comma" shape has become a well-recognized stage in the development process.

Hilda reached hurricane intensity (winds >74 mi./hr.) at about 16 GMT, Sept. 30, 1964. Precluding an earlier attainment of hurricane status was the island of Cuba, whose land mass has produced similar effects on previous occasions (Lateef and Smith [8]).

As indicated in figure 23, hurricane Hilda was a large, strong, deepening vortex almost centrally located in the Gulf of Mexico at 00 GMT, October 1. The central pressure had fallen to approximately 965 mb. and maximum winds were about 90 mi./hr. At 200 mb. (fig. 24), a large anticyclonic circulation dominated the whole Gulf region, except for the small cyclonic circulation immediately above the hurricane. The shear line of previous days appears to have been obliterated but the data do not preclude the possibility that some remnants remained east of the small cyclonic center aloft. Whether the disappearance of the shear line and the explosive deepening were pure coincidence is not determinable; other factors conducive to this deepening have been cited. The thickness pattern (fig. 25) leaves no doubt that a large warm mass of air at upper levels filled the Gulf region and caused well-marked anticyclonic shear winds everywhere but on the Mexican Gulf Coast.

Figure 26 presents the 200-mb. streamlines for 12 GMT on the 1st, just before Hilda reached its minimum central pressure of 941 mb. The combination of flight and synoptic data affords better than average coverage for streamline analysis. Hilda maintained a cyclonic circulation up through the 200-mb. level and the data present a classic example of the turning of this flow into anticyclonic outdraft. Of particular interest is the outdraft structure over the western Gulf where westerly winds were impinging on the upper level anticyclone. Despite the rapid turning of the winds (at a level where small irregularities are not too common) one could view the analysis as a textbook solution of how the outdraft would be disturbed by the intrusion of westerlies.

The satellite view of Hilda (at just about its deepest stage) and the corresponding nephanalysis are presented in figures 27 and 28. The now familiar appearance—much like that of a spiral nebula—is best shown in figure 29 which is an enlargement (not a mosiac) of a single frame of the storm. The orientation of the outflow cirrus streams (fig. 28 and 29) now match the 200-mb. streamflow quite closely northeast of the storm center, as they should in view of the small difference in synoptic times. Of special interest is the fairly well-marked eastern edge of the cirrus shield. While the abruptness of the edge may have been exaggerated in figure 28, figure 29 suggests a very rapid transition from thick cirrus to no discernible cloud at all.

The well-marked western edge of the cirrus shield on a given side of the storm has been frequently noted by hurricane flyers and was well documented for hurricane Cleo of 1958 (LaSeur and Hawkins [7]), in which case the western edge of the shield was also marked by a pronounced suppression of low level cumulus activity. Similar well-defined, not necessarily western, edges and sometimes low level suppression also have been noted since that time. More recently, Merritt and Wexler [10] have described the cirrus shield and related its well-defined edge to the rapid anticyclonic turning of the wind in the outflow layer until the flow becomes approximately tangential. While we have no desire to take issue with this description, we also have found well-defined cirrus edges along shear lines, as shown in figure 11. This type of pattern also has the generally required characteristics to produce sharp cirrus edges. Fett [2] has inferred that subsidence is occurring through the action of a "major

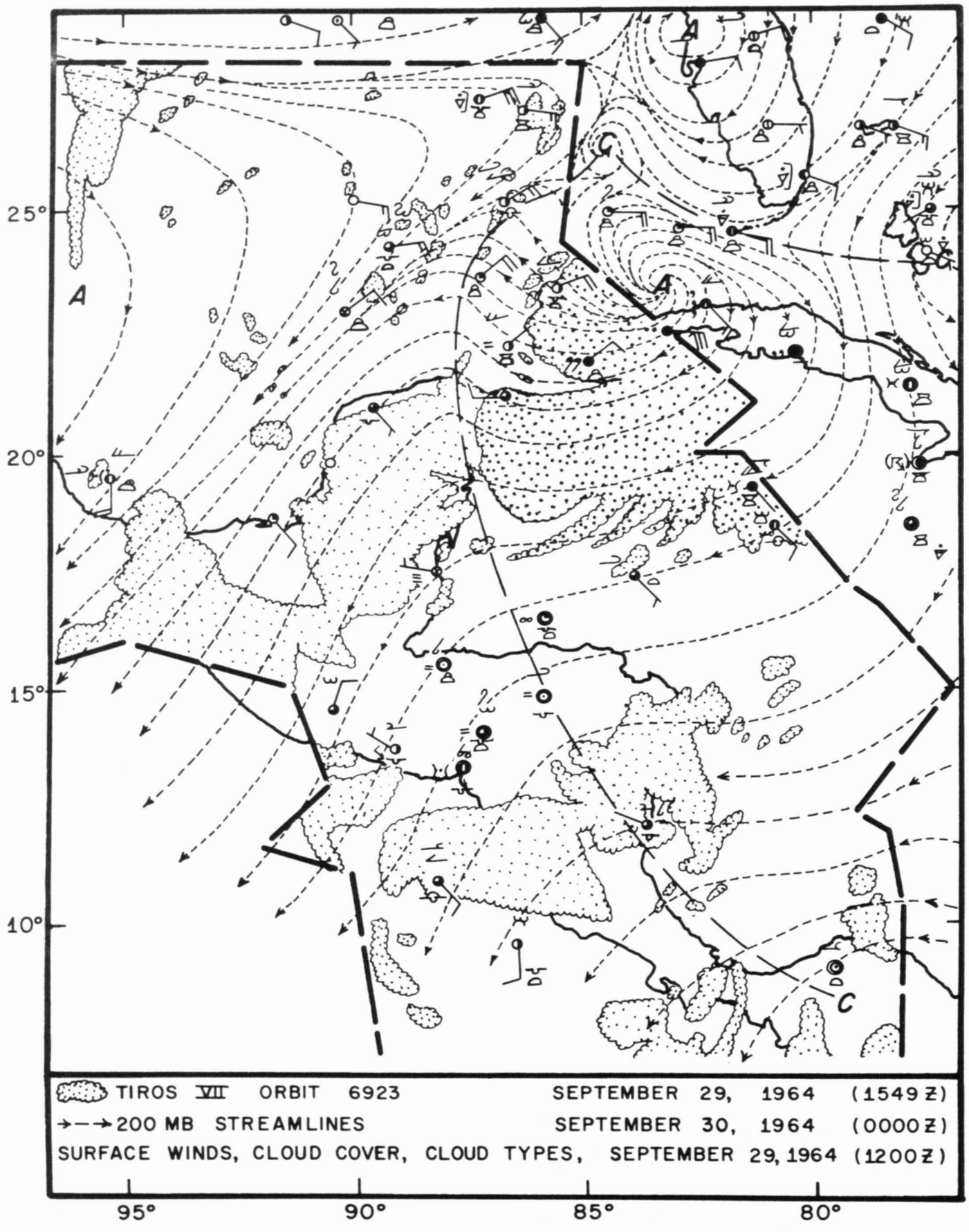

FIGURE 20.—The tail of the comma is well oriented with regard to the upper level outflow.

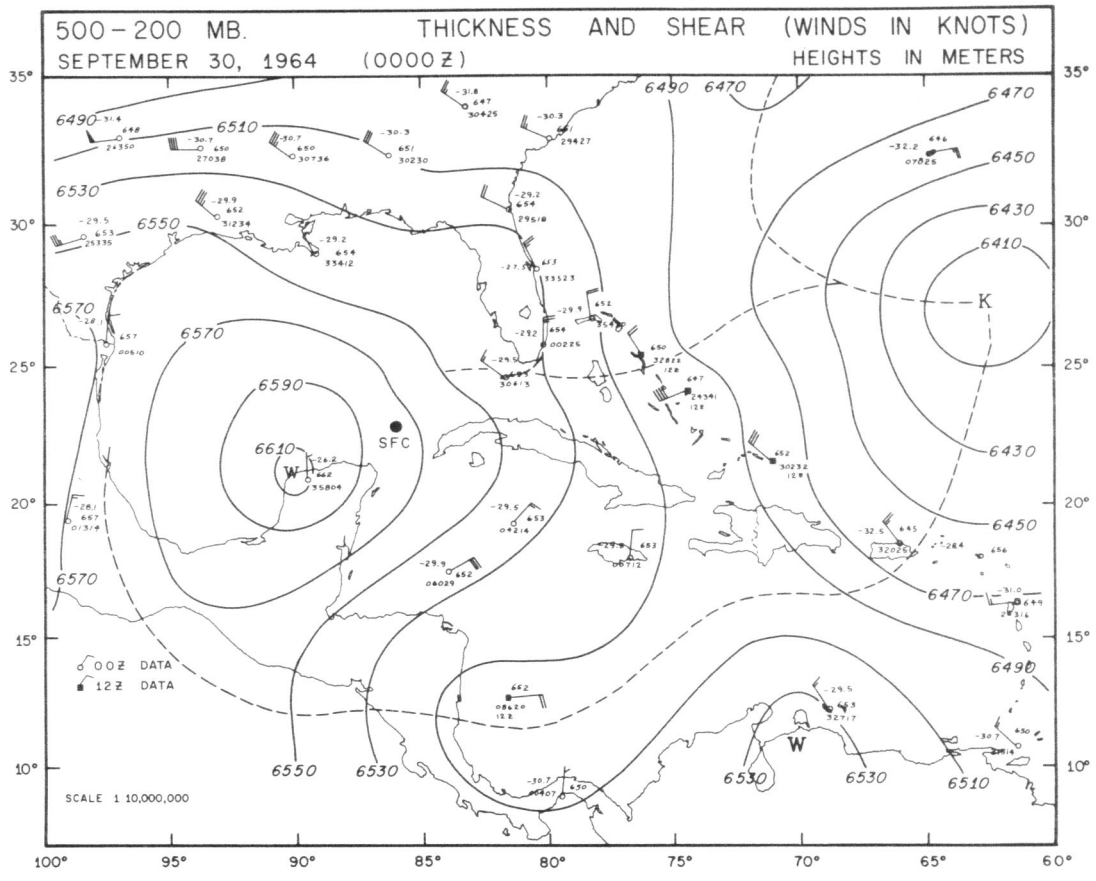

FIGURE 21.—Lack of data prohibited more detailed analysis of thickness over the storm area, but there is little doubt of the larger scale pattern.

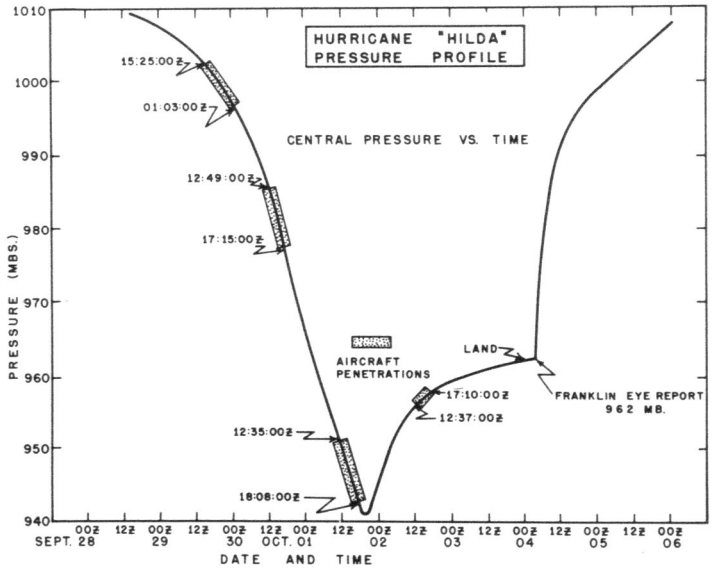

FIGURE 22.—A plot of the central pressure of hurricane Hilda against time, showing the times of aircraft reconnaissance. Note the extremely rapid filling after the eye went ashore.

subsiding branch of the hurricane's circulation"—and that this mechanism accounts for the sharp annular edge of the cirrus canopy. That such subsidence comprises a *major branch* of the hurricane circulation seems doubtful because the temperature effects of such circulation should be apparent and this has not proven to be the case. Nevertheless, divergence must accompany increasing anticyclonic turning in the outflow layer. When the air has "turned" sufficiently so that it is flowing in an approximate tangential path, then air from another, possibly dryer, source must flow parallel to it (on the left). Many sharp cirrus edges may arise in this fashion and limited subsidence may occur beneath the area of divergence. In the outflow layer where anticyclonic turning of the winds is no longer appreciable, it is difficult to see any marked subsidence that might terminate the cirrus canopy.

Merritt and Wexler [10] have made exploratory calculations as to the amount of descent required to evaporate reasonable amounts of ice in what is assumed to be a typical cirrus canopy. Although a limited amount of subsidence may well occur on the edges of the cirrsu canopy, we are reluctant to accept this mechanism as the only significant one. One reason is that the outer edges of the cirrus canopy have frequently been at quite high altitudes. Certainly the base of the cirrus shield occurs at lower and lower altitudes as a storm is approached. In addition, once the jet research aircraft enters the cirrus it seldom emerges until entering the eye, i.e. none of the flights suggests that the cirrus occurs at lower elevations at greater radial distances (on occasion, the jet does not emerge even in the eye). Consequently, we are inclined to favor the mixing of saturated cloud shield air with drier

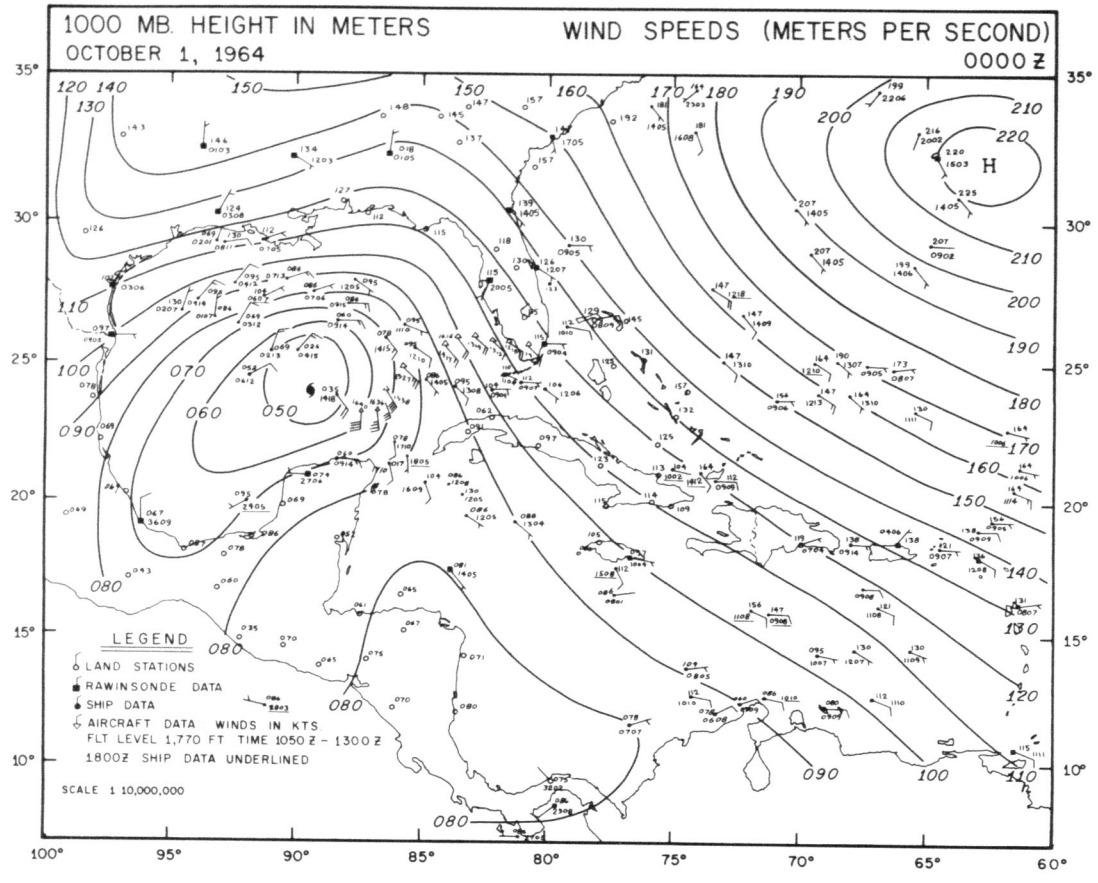

FIGURE 23.—Hurricane Hilda deepening rapidly near the center of the Gulf of Mexico.

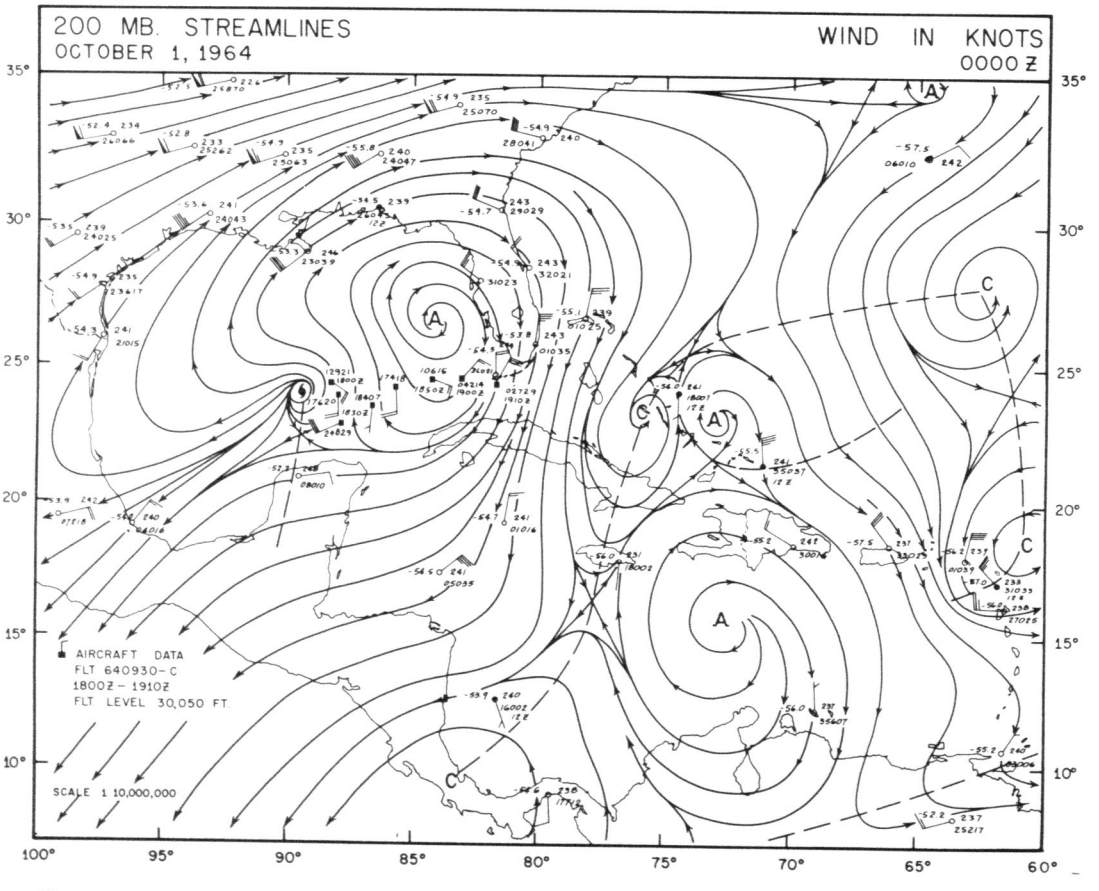

FIGURE 24.—200-mb. streamlines showing the outflow pattern associated with hurricane Hilda.

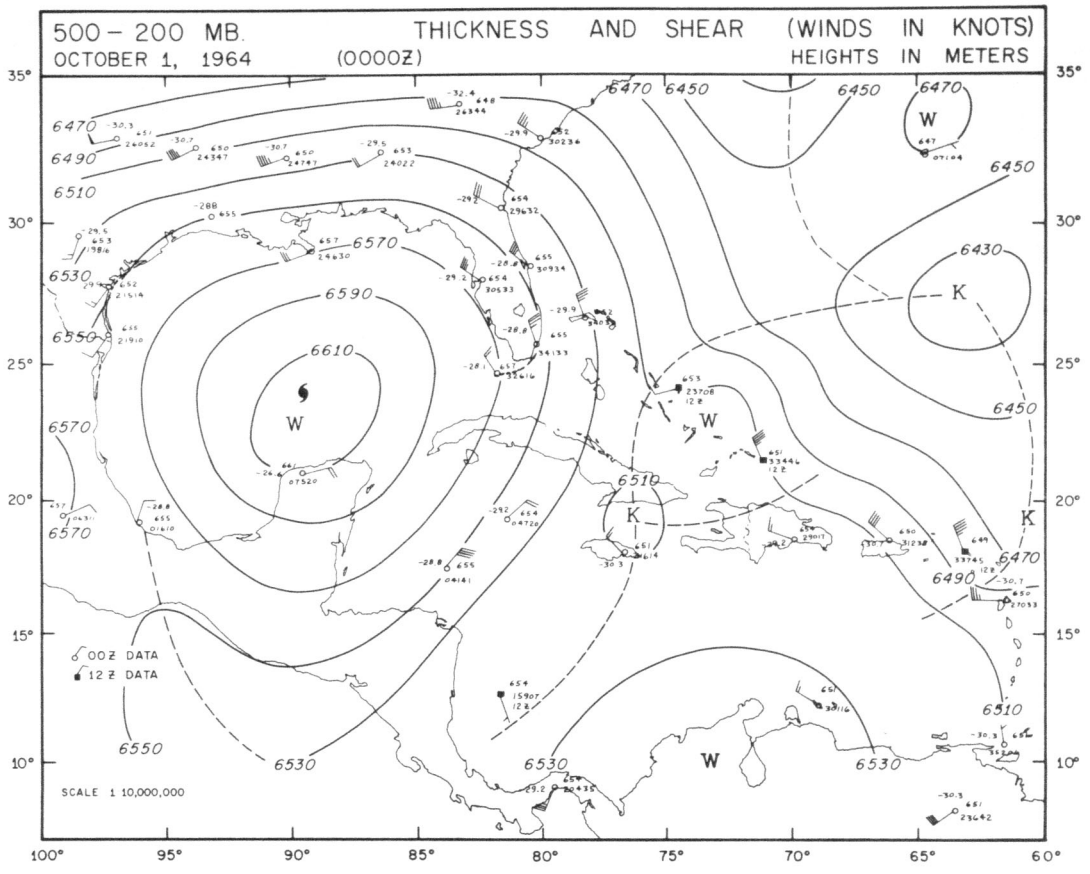

FIGURE 25.—The only shear winds that do not reflect the prevailing upper level warm pool accompanying Hilda over the Gulf are the weak winds at Vera Cruz, Mexico.

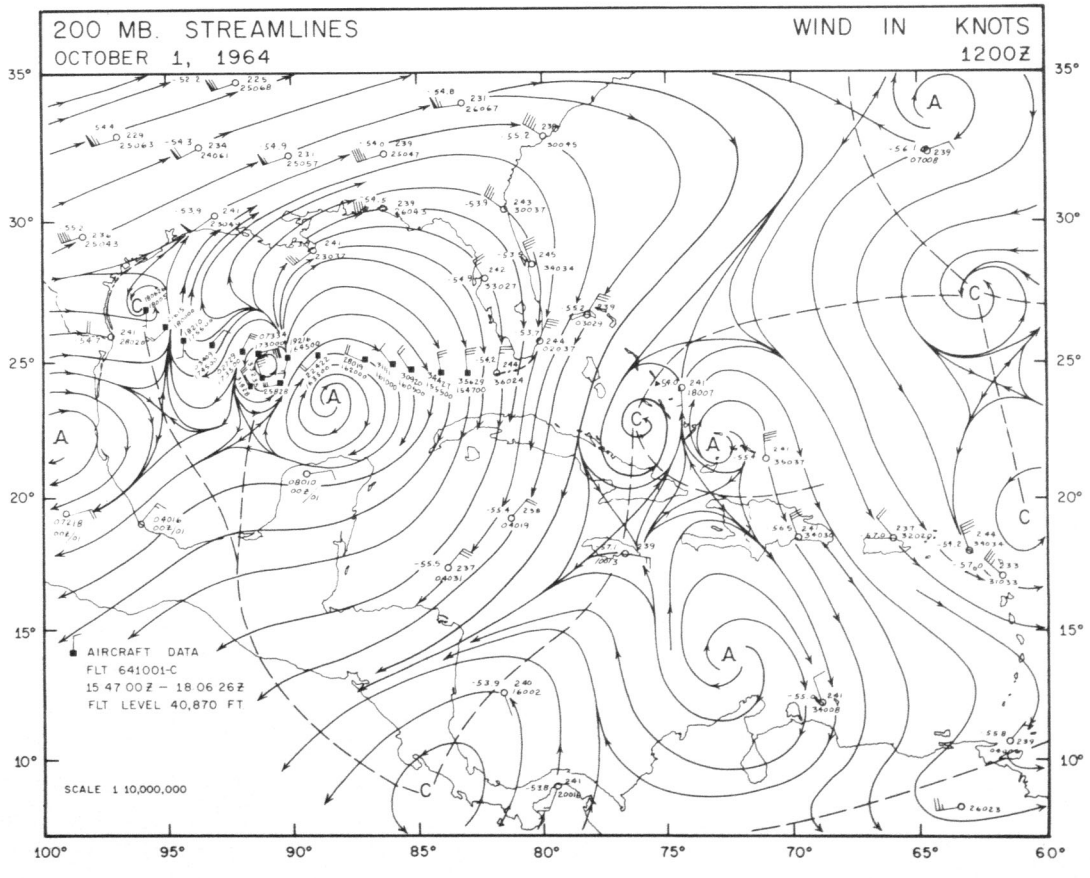

FIGURE 26.—Outflow pattern of hurricane Hilda (at 200 mb.) as detailed by aircraft winds.

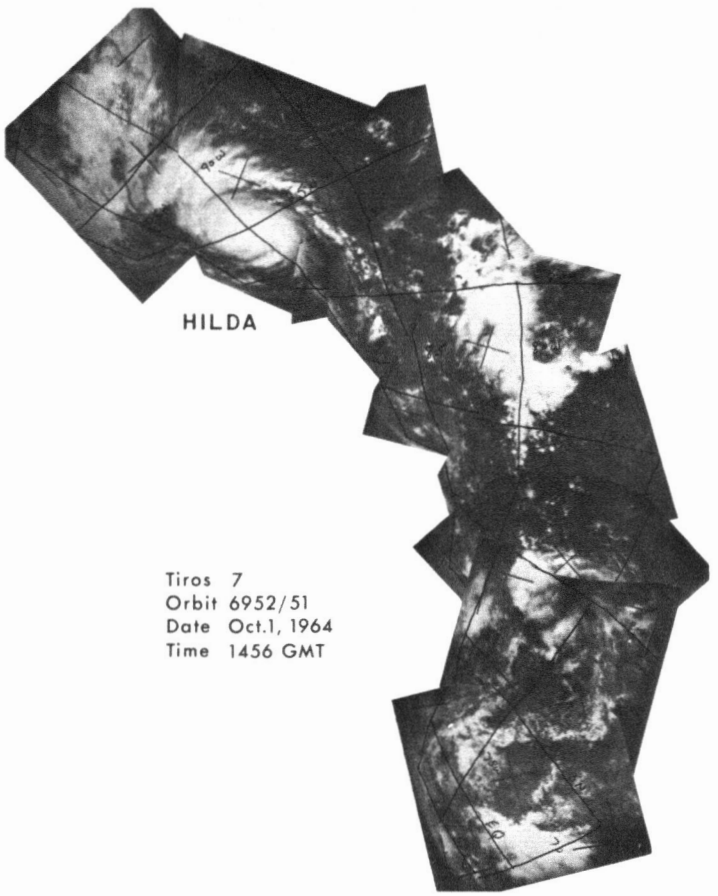

FIGURE 27.—Mosaic of satellite photographs showing the fully developed hurricane Hilda at the time of the major aircraft reconnaissance effort.

air (above and below) as an additional means by which the cirrus shield is thinned. However, in the straighter outflow currents thin sheets and patches of cirrus have been observed where the satellite pictures indicate little or none. In Hilda, on October 1, the time lapse films show some cirrus, even east of 85°W., or well past the "edge" of the outflow shield.

It does seem possible that to the west of the storm, where the anticyclonic curvature became most marked, subsidence may have played a more important role. Some of the harder cloud globules in figure 27 are undoubtedly composed of lower level clouds and their alignment is best associated with the surface winds plotted in figure 28. The enlargement of the best single frame photograph of Hilda, presented in figure 29, is an excellent example of hurricane "banding" and a fine illustration of how rapidly the solid cirrus canopy can *apparently* dissipate in the upper level "straight" outflow.[1]

[1] More recent experience with hurricane Beulah (1967) has demonstrated that the satellite photographs can indeed be misleading with regard to the edges of "blowoff" or outflow cirrus. Apparently, cirrus of a certain density is recorded by the photographs quite readily while cirrus of a not too distinguishable thinner texture goes almost unrecorded. In a flight from Miami while the outflow from Beulah was covering the Gulf of Mexico, it was noted that outflow cirrus was clearly discernible to the eye over the eastern Gulf but was impossible to discern on available satellite pictures. We submit that the "rapid dissipation" of cirrus *in the outflows* from the hurricane cirrus canopy is frequently exaggerated in satellite photographs and that marked and sudden subsidence is not needed to account for observed effects.

The first low level reconnaissance into the center of the storm took place September 29, shortly after it had cleared the island of Cuba. Hilda had acquired tropical storm status, with a central pressure of 995 mb. Figure 30 presents the low level flight data in profile form. The various parameters have been reduced to the 900-mb. surface for comparison with later figures. The 3.2-cm. radar vertical cross section is presented below the profiles for comparison. Maximum winds relative to the moving storm were 36 kt. about 13 n.mi. northeast of the center. To the northwest, maximum winds were 33 kt. about 16 n.mi. from the potential eye. Temperatures varied from 20 to 23°C. with the warmest air very near the storm center. The D-value profile for the 29th (fig. 30) shows that fairly well-marked gradients were already present. Computations of the gradient winds, using radii of trajectory curvatures, were carried out at 10-n.mi. intervals to see whether marked imbalances were present in the smoothed data. Results were inconclusive and showed balance within 10 to 20 percent maintained most of the time, with the actual winds subgradient in some instances and supergradient in others.

The radar cross section was prepared from the RDR-1D 3.2-cm. vertical cross section radar which pictures the precipitating elements in a plane perpendicular to the longitudinal axis of the aircraft.[2] Although the tops were not always stratiform and level, they were not wildly uneven and cumuliform in appearance. They varied from 14,000 to 16,000 ft. for the most part, and the highest echo top was at 31,000 ft. Most were rather level and not cumuliform in structure. The top of this "even" echo occurs about where the bright band would be expected to be in this situation; i.e., near the 0°C. isotherm.

We have discussed these records with H. V. Senn who recently presented a paper on this subject [14]. He believes the top of the echo does coincide with the bright band and and that the effect is caused by the snowflakes in old cumulus structures settling down and either beginning to melt or otherwise acquiring a coating of moisture that enhances their radar reflectivity. On settling further they undoubtedly turn into drops and/or droplets which fall as rain or evaporate in falling, or are maintained aloft by a weak vertical updraft. Whether the visible cloud form in which the echo occurs should be characterized as cumuli- or stratiform in nature may be a moot point. The amount of stratiform clouds found in tropical storms and hurricanes is quite large if one considers the importance of the cumulus activity in the energetics of the storm. However, while the cloud material may be almost exclusively cumulogenitus, many layers of clouds are found in these storms. We would prefer to view the band as occurring in a deck, or decks of stratiform clouds. How high the visible deck extends is not known, but in the inner portions of the storm

[2] This radar has a very small antenna with a rather poorly defined beam. The side lobes of the main beam contain significant amounts of power and give rise to "spurious" echoes. Since most targets are within 10 mi. of the plane, many problems of interpretation arise in working with these records. The interpretations offered in this paper should be viewed with reasonable reservations.

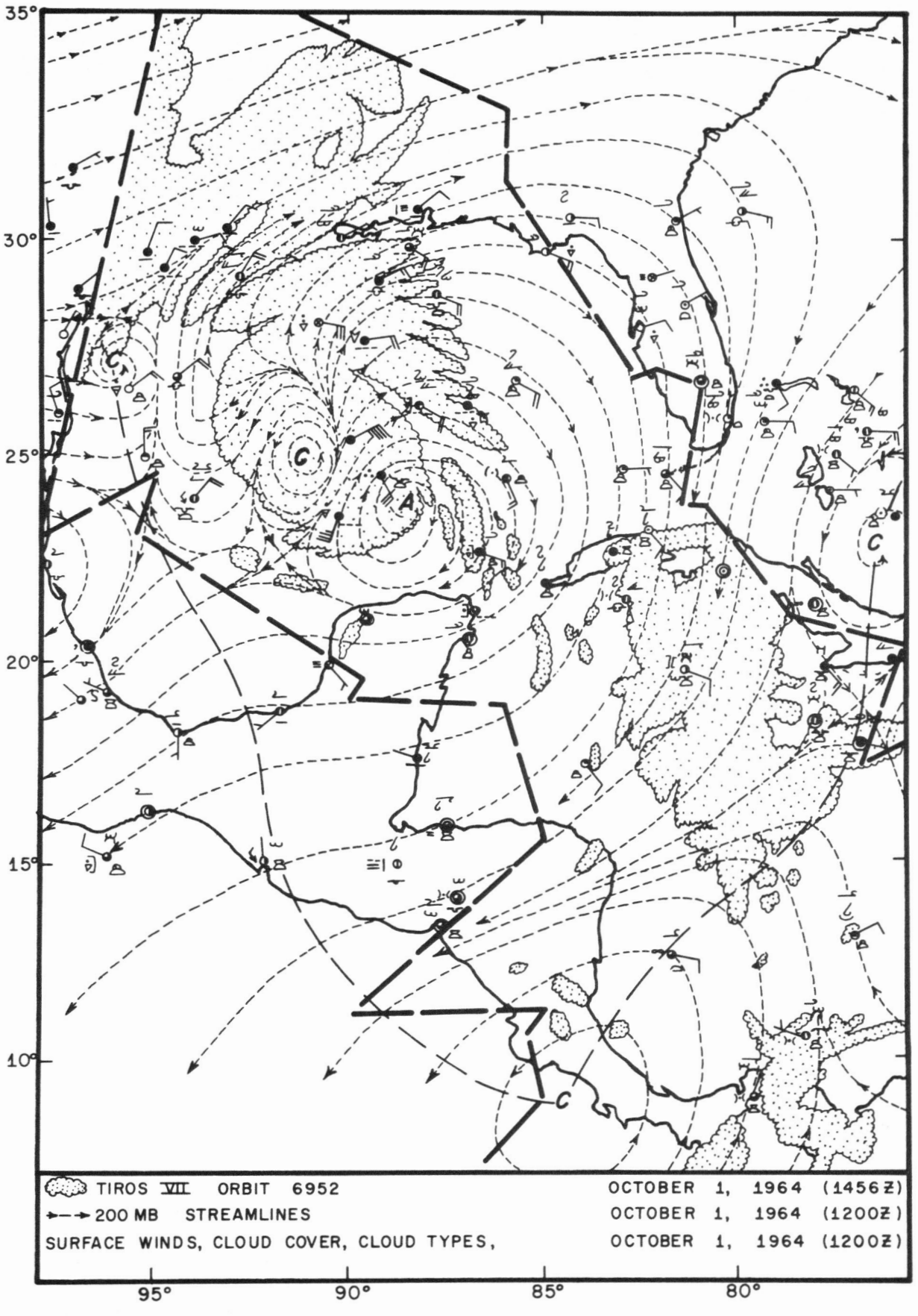

FIGURE 28.—Nephanalysis of figure 27 with upper level streamlines and surface observations. Note the rapid dissipation of the outflow cirrus.

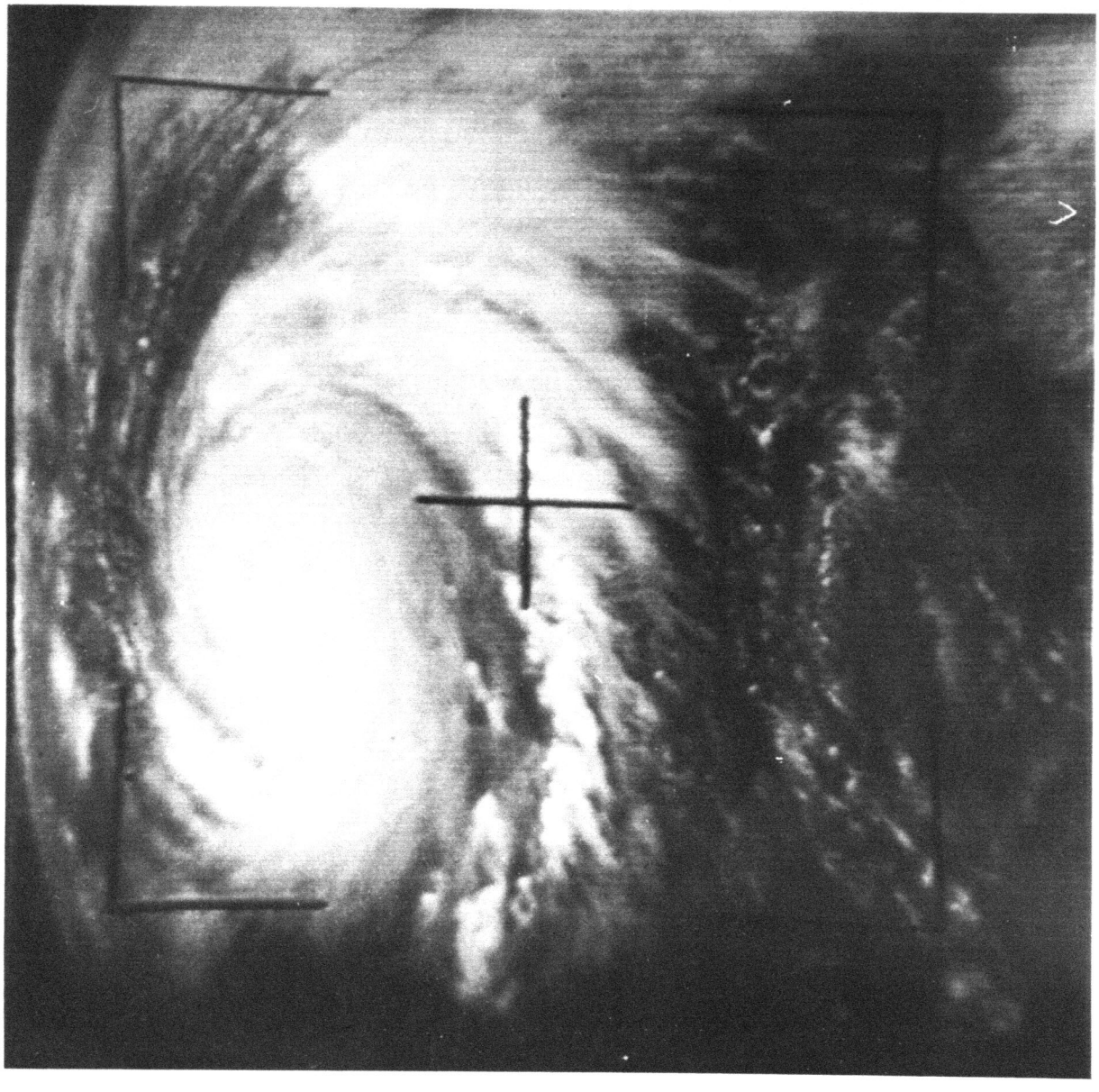

FIGURE 29.—Enlargement of the best single frame satellite photograph of hurricane Hilda.

it presumably extends to the top of the cirrus level, which seldom can be topped at 35,000 ft. In Hilda, on the 1st, the high level jet was in dense cirrus practically all the time it was within 100 mi. of the eye; so the cirrus canopy extended well above 40,000 ft. and may have contained cumulonimbus towers to comparable heights.

Some small support for this interpretation of the echo tops might be found in the change in altitude with radial distance from the storm center. Since the hurricane is a warm core disturbance, the bright band should be found at increasing elevation near the center. Some years ago the senior author of this paper suggested the possibility of estimating the strength of a hurricane through the altitude of the bright band near the wall cloud. The concept is based on the reasoning that the warmer the core, the lower the central pressure, the more intense the storm, and the higher the bright band should be. Sufficient data were not available at the time for further development of this idea. In the case of Hilda, there was only a weak suggestion (fig. 30) that the storm at this stage was already warm core; i.e., the bright band was somewhat higher near the eye. Difficulties in reading the films more accurately preclude a more definitive statement. At low elevations the temperature differences between the storm core and the environs are frequently quite small. In this case the temperatures at 60 mi. out averaged about 21.5°C., while in the storm center they averaged about 22°C. This is too small a temperature difference to be relied on to indicate the presence of a warm core or a cold core at upper levels. The bright band in figure 30 does seem to occur at slightly higher elevations as the core is approached; 60 mi. out, it appears at about 14,000 to 15,000 ft., while 10 mi. out on the northwest side it apparently is located near 16,000 ft.

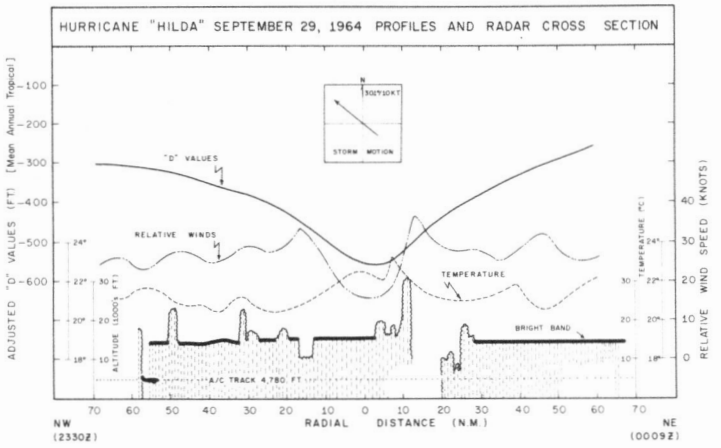

FIGURE 30.—Cross sections of *D*-values, wind speeds (relative to the moving storm), temperatures, and radar structure. This flight was made by low-flying aircraft late on September 29. Much of the radar return suggested precipitation falling from the bright band.

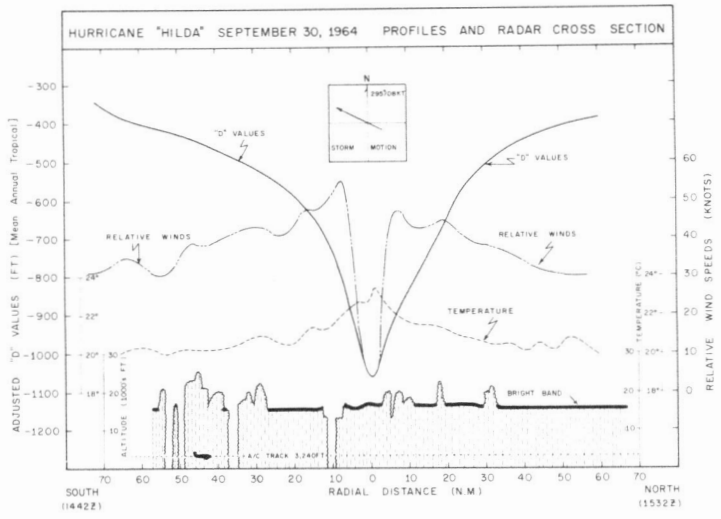

FIGURE 31.—Same as figure 30. The storm was now better organized with steeper *D*-value gradients, a concentration of high wind speeds near the center, and, even at these low levels, higher temperatures with decreasing radius. The bulk of the precipitation again appears to fall from the region of the bright band.

On the basis of this observation we might conclude that the tropical storm was most probably of warm core structure at this stage.

It is obvious from figure 30 that the inner core of the tropical storm was not filled with towering precipitating cumulus. In fact, the areas in which cumulus activity dominated the scene, obliterated the bright band, and led to a breakup in the stratiform regime were not predominant. The greater part of the inner core (inner 60 mi.) was stratiform in character. Very few radar echoes went to 20,000 ft. and only one was logged above 30,000 ft. Although this profile does not represent a complete cloud survey or census, it is also representative of the other passes. From all other passes only two other echoes that reached the 30,000- to 32,000-ft. level were found. Presumably, this radar "sees" raindrops and possibly cloud

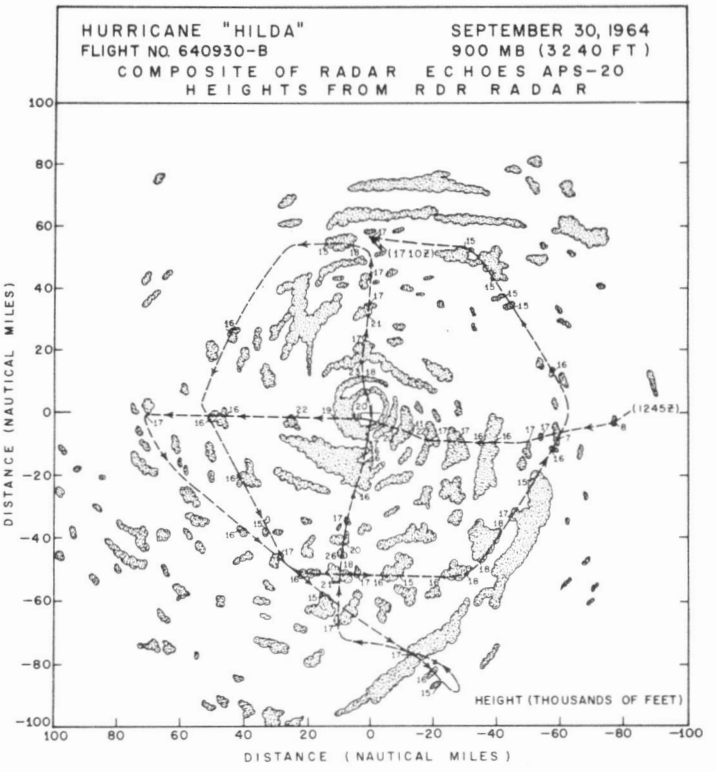

FIGURE 32.—The 10-cm. APS-20 radar was used to composite the more stable of the radar echoes depicted on the time lapse film. The echoes do not necessarily reflect every RDR-1D echo.

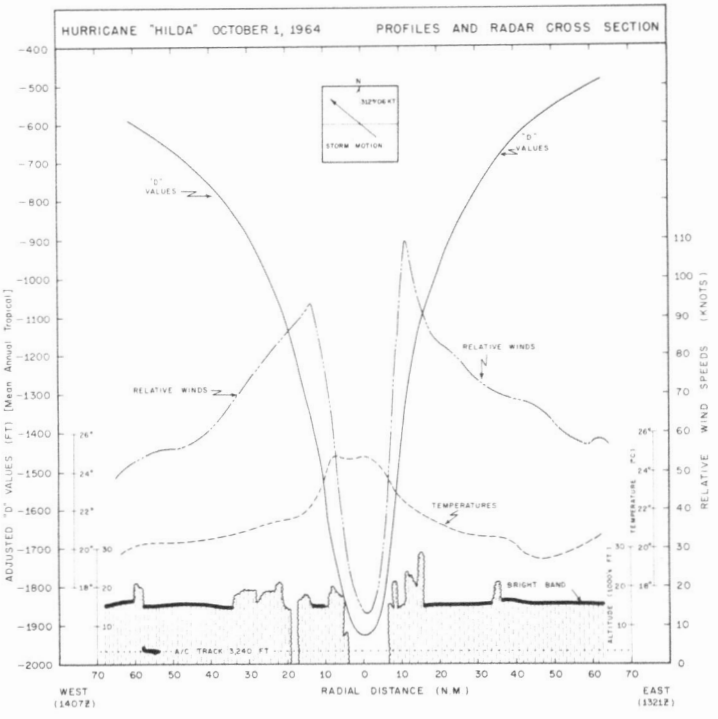

FIGURE 33.—Classical hurricane profiles on October 1 when Hilda was close to maximum intensity.

droplets or ice crystals at ranges of 10 mi. or less. Hence, it is likely that visible cumulonimbus clouds rose to considerably greater heights but active precipitation was not falling from these heights. In any event there was in

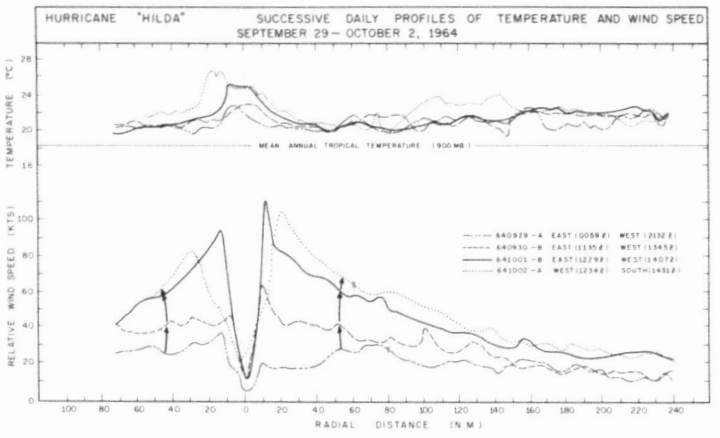

FIGURE 34.—Profiles showing the nature of the changes of temperature and wind speed as Hilda intensified and then relaxed slightly.

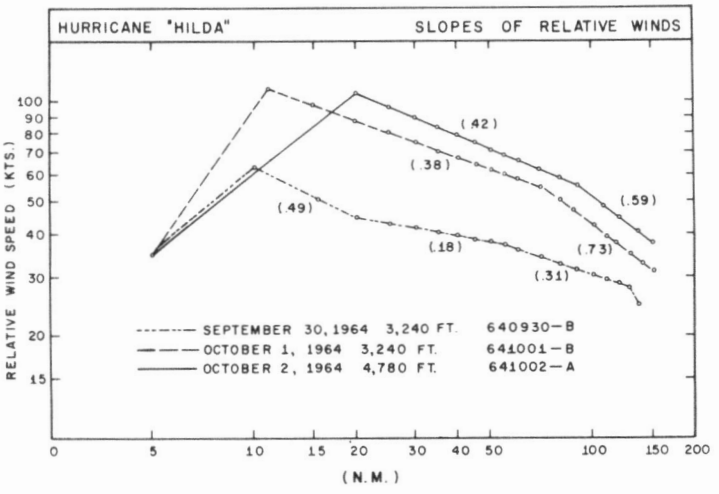

FIGURE 35.—Profiles of relative wind speed on a log-log plotout. The outer slopes were not constant even on the 1st and 2d when Hilda was a fairly typical hurricane.

all likelihood no copious supply of supercooled liquid water available in the form of *raindrops*.

On September 30, another low level survey of the storm was made by research aircraft. Figure 31 presents, in a format similar to the preceding figure, some of the data gathered. The wind speeds relative to the moving center were both stronger and better organized than on the 29th. Maximum relative winds were 56 kt. on the south side and 48 kt. on the north side. On either side of the maxima the winds decreased outward with shears much stronger than those in evidence a day earlier. As would be expected, the *D*-value gradient had also increased significantly, particularly in the region of maximum winds. There was some further evidence of warming in the core in that the temperature difference from the 60-mi. range to the center was now more than 2°C.

The 3.2-cm. radar cross section was notable for the extensive precipitation encountered at flight level. In accordance with this evidence of the stratiform nature of the cloudiness, the echo tops on this radar were relatively even over much of the traverse. Even where cumuli-

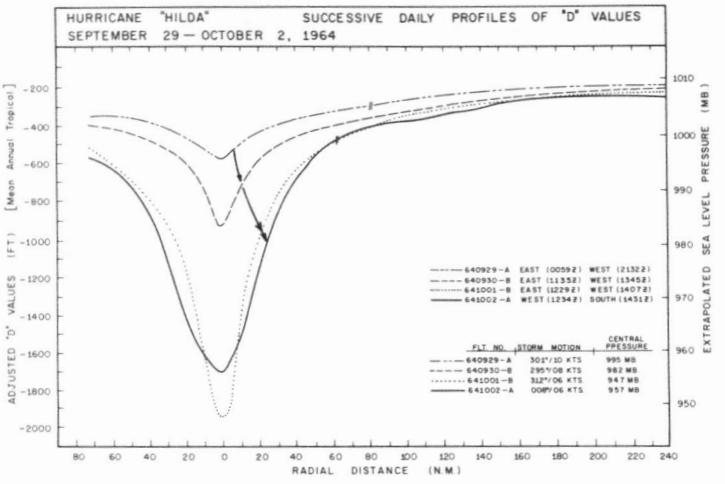

FIGURE 36.—Successive profiles of *D*-values as Hilda deepened from about 1000-mb. central pressure to 947 mb. and then filled slightly.

form activity prevailed the radar echoes did not penetrate to very impressive altitudes. The extreme height, found nearly 70 mi. to the north, was 27,000 ft. An extensive area of cumulus activity occurred from about 27 mi. to at least 55 mi. south of the center. There is a definite suggestion in the data that the altitude of the bright band increased towards the core on the south side of the storm despite the prevalence of cumulus activity. On the north side a somewhat similar trend was noticed, but it was not particularly well marked. The highest echo logged on this pass did not reach 30,000 ft. Figure 32 shows the PPI presentation of the more persistent radar echoes composited on the basis of film from the APS-20, 10.4-cm. radar set. These echoes were composited over a time interval of some 4½ hr. and comprise only the harder core echoes that were distinguishable from the sea return. Where both the APS-20 and RDR-1D obtained data from the same meteorological target the extreme height of the echo return on the 3.2-cm. set was tabulated (in thousands of feet) at the appropriate location. Because of the difference in wavelength and the differences in compositing there are noticeable differences between the radar cross section in figure 31 and the PPI composite of figure 32. In retrospect, it seems somewhat surprising that despite the evident growth and superior organization of the storm, little significant change in radar structure had become apparent between the 29th and the 30th. It should be emphasized at this point that the visible clouds undoubtedly extended to much higher levels.

On the succeeding day, October 1, Hilda was a full-fledged hurricane, and the profiles of figure 33 are of typical hurricane structure. Winds reached their maximum some 11 to 14 mi. from the center of the eye. The highest wind speed (relative to the moving hurricane) was 110 kt. Speeds peaked sharply at the maximum and showed reasonable anticyclonic shears with increasing radius. Even the low level temperatures showed fair evidence of the warm core structure; they rose from about 20°C. at 60 mi. out to more than 24°C. in the eye. It is possible, of course, that the outer temperatures were depressed in the

falling rain, a characteristic not uncommon in vortex thermometry and usually estimated at less than 2°C. (Hawkins et al. [6]). The D-values showed the deep V expected of a mature hurricane with maximum D-value gradients of the order of 175 ft./10 n.mi. At these latitudes this corresponds to a geostrophic wind in excess of 900 kt. The radar cross section shown in figure 33 suggests a significant increase of cumulo-type activity in the inner 20 to 30 mi. Echo tops are less than 30,000 ft. Nevertheless, broad areas are still dominated by stratiform structure with the bright band much in evidence, but there is no conclusive evidence indicating the elevation of the bright band with decreasing radius.

Successive daily profiles of temperature and wind speed are presented in figure 34. In some cases the "approach leg" (from 70 to 240 mi.) was not a direct precursor or successor to the inner leg in time or space, so the overall profiles have been composited where necessary; no serious inconsistency is thought to have resulted from this procedure. Profiles for October 2, when the storm had begun to weaken, are also included. No significant temperature changes occurred at this low level from the 29th to the 30th, when the storm was deepening slowly, but there was significant warming in the core from the 30th to the 1st as rapid deepening took place. Even after the hurricane had filled slightly on the 2d, temperatures in the eye remained high and a curious anomalous center of warmth was located just within the southern eye wall. The mean annual tropical temperature at 900 mb. is 18.3°C. and the temperatures associated with the inner and outer circulations of hurricane Hilda were without exception higher than this normal value.

The wind speed profiles (fig. 34) show a fairly regular transition. From the 29th to the 30th there was little change in speed at radii greater than 150 n.mi. Within this radius, however, winds (relative to the moving storm) generally increased, with a slight suggestion that there was a small diminution in the radius of maximum wind. The significant increase in maximum wind speeds from the 30th to the 1st was not accompanied by a decrease in the radius of maximum winds. On the contrary, the radius at which the maximum winds were found definitely increased. By observation time on the 2d, the maximum winds had decreased and the radius of maximum winds had expanded significantly. Also, there appeared to be (on the 2d) an asymmetry in the wind field accompanying the asymmetry in the temperature field cited previously.

If one assumes for the moment (Riehl [12]) that the potential vorticity is conserved in the inflow layer and that the drag coefficient is constant, then

$$rv_\theta^2 = \text{const. or } v_\theta r^{1/2} = \text{const.}$$

Various investigators have examined the wind profiles in order to determine the appropriate value of m in the equation $v_\theta r^m = \text{const}$. Riehl [12] has cited a number of storms in which m equaled 0.5 over significant portions of the wind profile. These were smoothed profiles which had been meaned azimuthally. Although we have serious reservations about the constancy of the drag coefficient in hurricanes, we have computed the values of m for the subjectively smoothed wind profiles shown on the right side of figure 34. The results of these computations (fig. 35) show that it is difficult to characterize the wind profile from the maximum wind out to the periphery by the use of a constant exponent for the radius, r. On the 30th, just before Hilda reached hurricane status, at least four values of m were required to describe the profile out to 150 mi. On the 1st, as the storm approached its maximum depth, the profile seemed simpler although for the region from the maximum wind out to 70 n.mi. the value of m was only 0.38. The difference between this value and that of the succeeding day (0.42) is probably not significant. In general, the slope of the profile seemed to increase as the storm intensified, as was also found by Riehl in his study of hurricane Daisy.

In figure 36, the successive D-value or pressure profiles have, of necessity, been composited in the same manner as those for temperature and wind speed. It appears that the area of significant deepening extended out only about 80 to 100 n.mi., a relatively small area in view of the large range in central pressures, i.e., from 995 to 947 mb. Major deepening occurred from the 30th to the 1st as previously mentioned. From the 1st to the 2d the vortex seems to have "expanded" rather than "filled." The central pressure was higher on the 2d but pressures were lower in the annular ring from about 10 to 40 n.mi. out from the center of the eye. This type of change is not unlike that which Project Stormfury effort hopes to achieve by hurricane seeding.

3. SUMMARY OF THE GENESIS OF HURRICANE HILDA

The origins of hurricane Hilda appeared to be associated with a mass of clouds moving westward from the south central portion of the western Atlantic to the Greater Antilles. Because of scarcity of data, it was not feasible to satisfactorily relate the cloud mass to a unique feature of the circulation. Long before Hilda became a hurricane, an easterly wave formed and began to deepen over the warm ocean surface. The wave was accompanied by extensive shower activity and a considerable release of latent heat in the 500- to 200-mb. layer. This heat, in turn, seemed to be associated with the development of further anticyclonic circulation at higher levels and further enhancement of the upper level divergent mechanism. Deepening was at a moderate rate at first but accelerated after the disturbance moved clear of the island of Cuba. Throughout the period of aircraft surveillance, a large areal proportion of the precipitation seemed to fall from stratiform clouds (undoubtedly of cumulus origin) with a well-marked bright band. Radar echoes did not extend to great heights at any time up through October 1—the highest was of the order of 32,000 ft. Visible clouds were of greater vertical extent than this. The final deepening was mainly over an area

relatively close to the storm core and was accompanied by a marked increase of cumuliform vs. stratiform radar echoes in the area surrounding the eye.

The genesis of Hilda proved in no way an exception to the general concepts of such events as they are currently accepted at the National Hurricane Center. These precepts include:

1) A preexisting disturbance at lower levels with low level inflow. In this case, the easterly wave was of recent origin and may have appeared first at midtropospheric levels.

2) A relatively warm ocean surface. The fact that major deepening occurred only after the storm cleared Cuba is not inconsistent with this requirement.

3) The presence (or simultaneous development) of a divergence mechanism aloft consistent with the low level inflow. The upper level anticyclone appeared to satisfy this requirement most admirably.

4) General warmth in the upper troposphere from 500 to 200 mb. The thickness patterns give adequate evidence of increasing temperatures in this layer. These temperature increases are in turn attributed to the release of latent heat in the showers that accompanied the disturbance.

The hypothesis that formation is favored in the areas of minimal shear (Gray [5]) is being further evaluated. Probably the most surprising aspect of Hilda was the lack of evidence on the vertical cross section radar of deep, penetrating cumulus buildups. The area dominated by cumulus activity was, as expected, and as is usually the case, quite small. But the lack of radar target echoes penetrating to 35,000 ft. or above was somewhat disconcerting although visible cloud towers to and above these levels may have been present. Further study and use of the 3.2-cm. vertical cross section radar is necessary before any conclusions can be reached as to how representative and valid these observations on the storm's radar structure may be.

ACKNOWLEDGMENTS

The data required special processing and editing, which was carried out under the direction of Mr. B. M. Lewis. Satellite photographs were made available by Mr. C. Ericson of NESC. Most of the special plotting and a number of machine programs for detailed computations were executed by Mrs. M. Kirkland. Mrs. R. Sherrill has assisted in the radar interpretations. We are indebted to Dr. S. Rosenthal for many interesting discussions, to Dr. B. Miller for some of his material on drag coefficients and to Dr. R. C. Gentry for advice and encouragement. We would be remiss not to mention the cooperative help of our illustrator, Mr. R. Carrodus, our photographer Mr. C. True, and our typists Miss D. Nejman, Mrs. B. True, and Miss M. Johnson. Last and by no means least, without the dedicated cooperation of the Research Flight Facility many of these data would never have been gathered and much of this and the following papers would have been impossible.

REFERENCES

1. G. E. Dunn and Staff, "The Hurricane Season of 1964," *Monthly Weather Review*, vol. 93, No. 3, Mar. 1965, pp. 175–187.
2. R. W. Fett, "Aspects of Hurricane Structure: New Model Considerations Suggested by TIROS and Project Mercury Observations," *Monthly Weather Review*, vol. 92, No. 2, Feb. 1964, pp. 43–60.
3. R. W. Fett, "Upper-Level Structure of the Formative Tropical Cyclone," *Monthly Weather Review*, vol. 94, No. 1, Jan. 1966, pp. 9–18.
4. N. L. Frank, "The 1964 Hurricane Season," *Weatherwise*, vol. 18, No. 1, Feb. 1965, pp. 18–25.
5. W. M. Gray, "Global View of the Origin of Tropical Disturbances and Storms," *Monthly Weather Review*, vol. 96, 1968.
6. H. F. Hawkins, Jr., F. E. Christensen, S. C. Pearce, and Staff, "Inventory, Use and Availability of National Hurricane Research Project Meteorological Data Gathered by Aircraft," *National Hurricane Research Project Report* No. 52, U.S. Weather Bureau, Miami, Fla., Apr. 1962, 48 pp.
7. N. E. LaSeur and H. F. Hawkins, "An Analysis of Hurricane Cleo (1958) Based on Data From Research Reconnaissance Aircraft," *Monthly Weather Review*, vol. 91, No. 10, Oct.–Dec. 1963, pp. 694–709.
8. M. A. Lateef and C. L. Smith, "A Synoptic Study of Two Tropical Disturbances in the Caribbean," *Institutes for Environmental Research Technical Memorandum-NHRL 78*, ESSA, National Hurricane Research Laboratory, Miami, Fla., Apr. 1967, 33 pp.
9. D. F. Leipper, "Observed Ocean Conditions and Hurricane Hilda, 1964," *Journal of the Atmospheric Sciences*, vol. 24, No. 2, Mar. 1967, pp. 182–196.
10. E. S. Merritt and R. Wexler, "Cirrus Canopies in Tropical Storms," *Monthly Weather Review*, vol. 95, No. 3, Mar. 1967, pp. 111–120.
11. E. H. Palmén, "On the Formation and Structure of Tropical Hurricanes," *Geophysica*, Helsinki, vol. 3, 1948, pp. 26–38.
12. H. Riehl, "Some Relations Between Wind and Thermal Structure of Steady State Hurricanes," *Journal of the Atmospheric Sciences*, vol. 20, No. 4, July 1963, pp. 276–287.
13. H. Riehl, "On the Origin and Possible Modification of Hurricanes," *Science*, vol. 141, No. 3585, Sept. 1963, pp. 1001–1010.
14. H. V. Senn, "Precipitation Shear and Bright Band Observations in Hurricane Betsy, 1965," *Proceedings of the Twelfth Conference on Radar Meteorology, Norman, Oklahoma, October 1966*, American Meteorological Society, 1966, pp. 447–453.
15. J. G. Taylor, *An Approach to the Analysis of Sea Surface Temperature Data for Utilization in Hurricane Forecasting in the Gulf of Mexico*, U.S. Weather Bureau Contract Nonr 2119(04) Dept. of Oceanography, Texas A&M University, College Station, 1966, 92 pp.
16. M. Yanai, "A Detailed Analysis of Typhoon Formation," *Journal of the Meteorological Society of Japan*, Ser. 2, vol. 39, No. 4, Aug. 1961, pp. 187–214.
17. M. Yanai, "Formation of Tropical Cyclones," *Reviews of Geophysics*, Washington, D.C., vol. 2, No. 2, May 1964, pp. 367–414.

[Received December 12, 1967; revised February 28, 1968]